# Neurodevelopmental defects in Dravet syndrome *Scn1a*$^{+/-}$ mice: selective rescue of behavioral alterations but not seizures by targeting GABA-switch.

Lara Pizzamiglio[1,2,3], Fabrizio Capitano[1,2,3], Evgeniia Rusina[1,2,3], Giuliana Fossati[4], Elisabetta Menna[4,5], Isabelle Léna[1,2,3], Flavia Antonucci[5,6*], Massimo Mantegazza[1,2,6,*]

1. Université Côte d'Azur, Valbonne-Sophia Antipolis, France.

2. CNRS UMR7275, Institute of Molecular and Cellular Pharmacology (IPMC), Valbonne-Sophia Antipolis, France.

3. Inserm U1323, Valbonne-Sophia Antipolis, France

4. IRCCS Humanitas Research Hospital, Rozzano, Milan, Italy

5. Institute of Neuroscience - National Research Council of Italy (CNR) c/o Humanitas Mirasole S.p.A, Rozzano, Milan, Italy.

6. Department of Biotechnology and Translational Medicine, University of Milan, Milan, Italy.

* Corresponding authors

Massimo Mantegazza, Institute of Molecular and Cellular Pharmacology (IPMC), University Côte d'Azur-CNRS UMR7275-Inserm U1323, 660 Route des Lucioles, 06560 Valbonne-Sophia Antipolis, France, Tel. +33 493953425, e-mail mantegazza@ipmc.cnrs.fr

Flavia Antonucci, Department of Biotechnology and Translational Medicine, University of Milan, Via Vanvitelli 32, 20133 Milan, Italy, Tel. Tel. +39 0250317095, e-mail flavia.antonucci@unimi.it;

Running title: Neurodevelopmental defects in Dravet syndrome mice.

The authors have declared that no conflict of interest exists.

Keywords: developmental and epileptic encephalopathy; GABAergic; epilepsy; autism; Nav1.1; sodium channel.

# Abstract

Dravet syndrome (DS) is a developmental and epileptic encephalopathy (DEE) caused by mutations of the *SCN1A* gene and characterized by seizures, motor disabilities and cognitive/behavioral deficits, including autistic traits. The relative role of seizures and neurodevelopmental defects in disease progression is not clear yet. A delayed switch of GABAergic transmission from excitatory to inhibitory (GABA-switch) has been reported in models of DS, but its effects on the phenotype have not been investigated.

In the *Scn1a*$^{+/-}$ mouse model of DS, we studied GABA-switch and neurodevelopmental defects before the onset of spontaneous seizures, and assessed their impact on epileptic and behavioral phenotypes performing specific treatments. We evaluated *in vivo* features performing behavioral tests and cellular/network properties performing ex-vivo electrophysiological recordings.

Rescue of GABA-switch with the drugs KU55933 (KU) or bumetanide improved cognitive/behavioral defects. However, the treatments had no effect on seizures or mortality rate. Moreover, we observed early behavioral defects and delayed neurodevelopmental milestones well before seizure onset.

Thus, we disclosed neurodevelopmental components in DS that selectively underlie some cognitive/behavioral defects, but not seizures, and provide evidence to the hypothesis that seizures and neuropsychiatric dysfunctions can be uncoupled in DEEs. They could be treated separately with targeted pharmacological strategies.

# Introduction

Developmental and epileptic encephalopathies (DEEs) are characterized by severe epileptic seizures with early-onset and a variable amount of underlying neurodevelopmental impairment that tends to worsen as a consequence of epilepsy, but it is difficult to discriminate the neurodevelopmental and epileptic components of the disease (1). Dravet syndrome (DS) is a severe DEE (2, 3) caused by heterozygous mutations of the *SCN1A* gene, which lead to loss of function of the $Na_V1.1$ voltage-gated sodium channel (4). Disease onset occurs during the first year of life with seizures triggered by fever or hyperthermia, which persist also in adulthood, and subsequent appearance of various other types of seizures with high rate of sudden unexpected death in epilepsy (SUDEP) (3, 5). Beyond the severe epileptic phenotype, DS is characterized by developmental plateauing with motor disabilities, cognitive deficits and neuropsychiatric symptoms, which often greatly contribute to the severity of the phenotype. The latter include anxiety, attention deficit hyperactivity disorder (ADHD), narrow interests, and impaired communication and social interactions, features that overlap with symptoms of autism spectrum disorder (ASD)(6–9, 3). Three stages have been proposed in the natural history of DS: febrile, worsening and stabilization (5). The available drugs are symptomatic treatments with limited efficacy and insufficient control of convulsive seizures, whereas there is not yet a treatment reported as clearly effective on cognitive/behavioral dysfunctions (3, 10). Heterozygous knock-out $Na_V1.1$ (*Scn1a*$^{+/-}$) mice recapitulate the human DS phenotype (11–13). Hyperthermia-induced seizures can be induced from around postnatal-day 15 (P15). Onset of spontaneous recurrent seizures is at around P20 with high SUDEP rate, as well as cognitive/behavioral defects, including autistic-like traits; in this period, which is equivalent to the human worsening stage, seizures are particularly frequent and mortality particularly high. A stabilization of the phenotype is observed after around P35, but cognitive/behavioral defects are permanent, as in patients. Mouse models have been instrumental for showing that $Na_V1.1$ loss-of-function, caused by DS mutations, induces reduction of sodium current and of excitability in GABAergic interneurons, leading to impaired GABAergic synaptic transmission (12, 14). This mechanism has been confirmed by numerous studies in different animal models and in patients, showing the pivotal role of GABAergic interneurons' dysfunctions in DS (11, 15–18).

The relative contribution of seizures and underlying neurodevelopmental impairments to the encephalopathy, in particular to neuropsychiatric features, is still debated in DS, as for other DEEs. In fact, some clinical studies highlighted mainly epileptic encephalopathy features, whereas others

showed developmental alterations even before the onset of epilepsy and reported that in some cases the severity of epilepsy and cognitive defects were not correlated (19–23).

Although hypoexcitability of GABAergic neurons is the most convincing pathological mechanism and therapeutic target in DS, the detailed molecular mechanisms underlying epilepsy and comorbidities, their causal relationships and the precise time window at which the different pathological features develop are still poorly understood, limiting the development of targeted therapeutic strategies. Interestingly, a recent study has shown that in a DS *Scn1a* knock-out mouse model the reversal potential of GABA-evoked currents is depolarized compared to WT mice between P13 and P21, consistent with a delay in the switch of GABAergic transmission from excitatory to inhibitory (i.e. GABA-switch) (24). However, the study has not investigated the overall effect of this dysfunction on the phenotype of the DS *Scn1a* model, although it has reported an effect on mortality in a model of sodium channel β1 subunit DEE (24), which is a different clinical entity compared to DS (1, 25, 26). Similarly, a depolarized reversal potential for GABA-evoked currents was observed in *Xenopus* oocytes transplanted with cell membranes obtained from autopsy brain tissues of Dravet syndrome patients, but the effect of this dysfunction on neuronal properties and on phenotype was not investigated (27).

The GABA-switch is a fundamental step of brain development that reflects the maturation time course of GABAergic signaling and depends on the electrochemical $Cl^-$ gradient, which is set by the relative expression of cation–chloride transporters NKCC1 ($Na^+$-$K^+$-$Cl^-$ cotransporter isoform 1) and KCC2 ($K^+$-$Cl^-$ cotransporter isoform 2). Its onset is normally around P8-10 in rodents and it is in general completed by P15 (28–30). Importantly, a delay in GABA-switch has been found in numerous models of neurodevelopmental disorders and it has been proposed as a therapeutic target in patients (31–33). Overall brain expression of $Na_V1.1$ starts around P8 in mice and homozygous *Scn1a*$^{-/-}$ mice die by P15 (12, 16), showing that $Na_V1.1$ loss of function can induce early effects. Thus, GABA-switch may be targeted in therapeutic approaches for DS, and early neurodevelopmental defects may be implicated in DS.

Here, we targeted GABA-switch in DS *Scn1a*$^{+/-}$ mice performing specific pharmacological interventions and assessing their effect on both epileptic and behavioral phenotypes, and investigated overall neurodevelopmental defects in the period before the onset of seizures.

# Results

**GABA-switch is delayed in DS *Scn1a*$^{+/-}$ mice.**

We evaluated the effect induced by the activation of GABA-A receptors on the spontaneous excitability of CA3 excitatory hippocampal pyramidal neurons in brain slices of P18-P21 *Scn1a*$^{+/-}$ mice, an age at which the GABA-switch should be accomplished and before onset of spontaneous seizures in this model. Hippocampal CA3 neurons have been used in numerous studies that have evaluated the kinetics of GABA-switch (29–33). We performed current clamp (I=0) electrophysiological recordings of spontaneous spiking activity in loose patch configuration, quantifying the modifications of spiking activity induced by the application of the GABA-A receptor agonist isoguvacine (10 µM) (34). We found a preponderant depolarizing response leading to increased excitability in pyramidal neurons of *Scn1a*$^{+/-}$ mice, whereas in WT littermates most of the cells showed a reduction of spike frequency, although the reduction did not reach statistical significance (Fig. 1A,B). These results confirm that the GABA-switch is delayed in DS mouse models, as it has been reported in a different DS *Scn1a* knock-out model measuring the reversal potential of GABA-evoked currents (24).

**KU55933 normalizes GABA-switch and decreases the excitatory/inhibitory ratio in *Scn1a*$^{+/-}$ mice**

A delayed GABA-switch has been implicated in numerous neurodevelopmental diseases (31–33, 35). We investigated its consequences on the overall phenotype and its importance as pathological mechanism in *Scn1a*$^{+/-}$ DS mice. We used two different pharmacological strategies, targeting the two chloride transporters that are responsible of the intracellular chloride homeostasis in neurons: KCC2, involved in chloride efflux, and NKCC1, involved in chloride influx. We exploited KU55933 (KU) which, blocking ATM kinase activity, acts on the GABA-switch by increasing the expression of KCC2 (36, 37), and bumetanide, a FDA-approved NKCC1 specific antagonist (38–40). The action of bumetanide has been reported in numerous studies, whereas KU is less characterized. Therefore, we investigated the effects of KU in *Scn1a*$^{+/-}$ mice *ex-vivo*.

We treated mice in the pre-epileptic period using intranasal delivery of KU (7,5 mg/kg) to efficiently cross the BBB and to target specifically and directly the central nervous system, as in (36). In order to compare littermate mice in electrophysiological recordings, we performed the treatment (two administrations every 72 hours) with sliding windows starting from P12-P15 and the recordings at P18-21; biochemical analysis was performed at P21 starting the treatment at P15 (Fig. 1C). The electrophysiological evaluation of the effect of the treatment was obtained measuring the effect

induced by the application of the GABA-A receptor agonist isoguvacine on the spontaneous spiking activity of CA3 pyramidal cells in hippocampal slices, which showed a rescue of the delayed GABA-switch that we observed in control conditions in *Scn1a*$^{+/-}$ mice (Fig. 1D-E). Western blot experiments showed that the dysregulation of the GABA-switch in *Scn1a*$^{+/-}$ mice was correlated to decreased expression of KCC2, which was normalized by the treatment with KU (Fig. 1F). Conversely, we found no changes in NKCC1 expression, neither in control nor upon KU treatment (Fig. 1G).

Notably, besides the GABA-switch (which is a postsynaptic feature), KU acts also on the overall kinetics of maturation of synaptic transmission and thus on the overall features of the network (36, 37). Thus, we evaluated the effect of KU on spontaneous GABAergic (sIPSCs) and glutamatergic (sEPSCs) post-synaptic currents in hippocampal CA1 pyramidal neurons of KU- or vehicle-treated *Scn1a*$^{+/-}$ mice, compared to untreated WT littermates (Fig. 2A). The properties of sIPSCs and sEPSCs depend on both synaptic properties and network excitability, allowing to evaluate the overall features of the network. We analyzed hippocampal CA1 pyramidal neurons because they have been investigated in numerous previous studies and are clearly involved in the pathophysiology of DS (41, 42). In vehicle-treated *Scn1a*$^{+/-}$ mice, we observed a reduced frequency of sIPSCs (Fig. 2B), as already reported in numerous studies of *Scn1a* loss of function. We also observed an increased frequency of sEPSCs (Fig. 2C), possibly induced by the reduction of IPSCs, leading to an increase of the excitatory/inhibitory ratio (Fig. 2D). We observed a small increase of sIPSCs and sEPSCs amplitude, which was not significant comparing mean values (Fig2E, F). The KU treatment decreased the frequency and the amplitude of sEPSCs (Fig. 2C and 2F), whereas we observed only minor effects on sIPSCs (Fig. 2B and 2E). Despite the small effect on sIPSCs, the KU treatment was sufficient to rescue the E/I ratio of the cells (Fig. 2D). Although this is an interesting result, it should be kept in mind that the E/I ratio is a general parameter, obtained from mean values, which does not reflect the actual dynamical relationship between excitation and inhibition in the neuronal network.

Overall, the KU treatment can rescue some of the dysfunctions that we observed, in particular the GABA-switch delay.

**Targeting GABA switch in Scn1a$^{+/-}$ mice has no effect on induced or spontaneous seizures**.

We performed *in vivo* experiments to evaluate the effect of KU and bumetanide on the epileptic phenotype of *Scn1a*$^{+/-}$ DS mice, because the two treatments can rescue GABA-switch targeting different mechanisms. We treated animals starting from P15 (Fig. 5A) with intranasal administrations of KU (7,5 mg/kg every 72 hours) as in (36), or with bumetanide (2 mg/kg IP daily),

method of administration that has been effectively used in numerous studies on different animal models of brain diseases (43–45). We began treatments at P15 to simulate clinical treatments, which do not start before the onset of the disease at the febrile stage. We initially evaluated the effect on hyperthermia-induced seizures at P21. Both treatments were ineffective in modifying the threshold temperature for seizure induction (Fig. 5B, D) or the severity of seizures, quantified using a modified Racine scale (Fig. 5C, E; see methods), which were similar to the values that we observed in control *Scn1a*$^{+/-}$ mice treated with vehicle. To further characterize the contribution of the developmental delay linked to GABA-switch on the epileptic phenotype in *Scn1a*$^{+/-}$ DS mice, we quantified in separated animal cohorts spontaneous convulsive seizures identified by semi-automatic analysis of high-resolution video recordings (46). This method allowed to avoid the surgical procedure for implanting electrodes for chronic recordings, which are difficult to implement at early ages, and permitted to chronically evaluate the animals for a long period starting from P15, the first day of the treatment. We performed video recordings for fifteen days (24/24h, 7/7d), from P15 to P30, on animals chronically treated with KU or bumetanide (Fig. 5A). Neither KU nor bumetanide reduced the frequency of seizures (Fig. 5F, I). We also analyzed the number of seizure clusters (we considered a cluster as two or more seizures with a delay of less than fifteen minutes) and found no changes in animals treated with KU or bumetanide compared to controls (Fig. 5G, J). Also, the two compounds had no effect on the survival rate of DS mice (Fig. 5H, K). Thus, neither KU nor bumetanide had effect on hyperthermia-induced or spontaneous seizures, showing that the long-lasting depolarizing effect of GABA does not play a crucial role on epileptogenesis or seizures generation in *Scn1a*$^{+/-}$ DS mice.

**Rescuing the GABA-switch delay ameliorates sociability, hyperactivity, and cognitive deficits in juvenile *Scn1a*$^{+/-}$ mice.**

Since cognitive/behavioral dysfunctions are a major issue in DS, we investigated whether the pharmacological rescue by KU or bumetanide of the abnormal GABA-switch could ameliorate the cognitive and behavioral deficits of *Scn1a*$^{+/-}$ mice. We began the treatment at P15, and we performed behavioral tests at P21 (Fig. 4A). We analyzed juvenile animals before the establishment of a strong epileptic phenotype to discriminate precisely the neurodevelopmental component involved in behavioral features from secondary effects induced by seizures.

We initially focused on autism-like features, assessing deficits in social interactions, which have been already reported in adult *Scn1a*$^{+/-}$ mice (11, 47). In the three-chamber test, *Scn1a*$^{+/-}$ male mice

had profound defects in social interactions already at P21. Notably, targeting GABA-switch with KU or bumetanide rescued this behavioral defect. Both WT and *Scn1a*$^{+/-}$ displayed no preference for the left or right chamber during the habituation period (Supplementary Fig. 1). However, when a stranger mouse was placed in one of the chambers, WT mice spent more time in close interaction with the stranger mouse than in the empty cage. Conversely, *Scn1a*$^{+/-}$ mice had no preference for the stranger mouse. Remarkably, both KU and bumetanide treatments rescued the impairment in social interaction (Fig. 4B, D). As already reported for adult mice (48), juvenile *Scn1a*$^{+/-}$ female mice did not show impairments in the three-chamber test (Fig. 4C).

Then, we tested cognitive features in juvenile *Scn1a*$^{+/-}$ mice using the Y maze spontaneous alternation test, which can be used to assess spatial working memory. Spontaneous alternation is a behavior driven by the innate curiosity of rodents for exploring previously unvisited areas and can be evaluated by allowing mice to explore freely all three arms of the maze. Moreover, the number of entries in each arm and the total distance traveled can be used for evaluating locomotor (hyper-) activity. We tested P21 *Scn1a*$^{+/-}$ mice treated with KU or bumetanide and compared them with WT littermates, considering males and females separately (Fig. 5). Both groups of control *Scn1a*$^{+/-}$ male mice displayed a statistically significant decrease in the percentage of spontaneous alternations compared to WT males (Fig. 5A, D). In contrast, performances of *Scn1a*$^{+/-}$ females were not different compared to WT female mice (Fig. 5G, J). Both male and female *Scn1a*$^{+/-}$ DS mice showed a higher number of entries in the arms of the Y maze (Fig. 5B, E, H, K) and covered significantly longer distances during exploration (Fig. 5C, F, I, L). These data are in line with previous reports of hyperactive behavior in DS mouse models (52,51,70), and show that hyperactivity can be already observed in the pre-epileptic period. As shown in Fig. 5A, treatment with KU did not improve the dysfunctions of *Scn1a*$^{+/-}$ males in spontaneous alternations. Although it did not reach statistical significance, KU treatment showed a loose trend towards the rescue of total distance traveled by males (5C) and a strong trend towards reduction of both the number of entries and the total distance traveled by females (Fig 5H, I). Notably, bumetanide rescued the reduced alternations, the number of entries and the total distance traveled of *Scn1a*$^{+/-}$ males (Fig. 5D, E, F). In *Scn1a*$^{+/-}$ female mice, bumetanide rescued the number of entries and partially improved the total distance traveled (Fig. 5K, L).

Therefore, targeting GABA-switch has an effect on autism-like features, spatial memory and hyperactive behavior in *Scn1a*$^{+/-}$ mice.

1 ***Scn1a*$^{+/-}$ mice display neurodevelopmental defects before seizures appearance**

2 Because delayed GABA-switch is implicated in early neurodevelopmental dysfunctions (31–33), we
3 investigated whether behavioral deficits in *Scn1a*$^{+/-}$ mice can be observed at early postnatal stages,
4 when $Na_V1.1$ is already expressed but before seizure onset. We quantified several developmental
5 milestones, in particular those frequently used for characterizing dysfunctions in animal models of
6 ASD (50, 51). We analyzed motor ability and coordination at P7 and P10-11 and found no differences
7 in righting reflex, grasping reflex, negative geotaxis, and gait (Fig. 6A-D). Olfactory detection and
8 motivation to reach the nest and mother is one of the earliest behavioral correlates of social
9 information processing, and a poor interest in reaching the home-cage bedding has been reported
10 in mouse models of autism and socially anhedonic syndromes (50–52). We performed the nest
11 bedding olfactory motivation test at P10-11. As shown in Fig. 6E, *Scn1a*$^{+/-}$ mice displayed significant
12 impairments in reaching the home cage bedding compared to WT, with no differences in the
13 average time taken to reach the nest, consistent with no dysfunctions in sensory and motor abilities.
14 Moreover, eye opening was delayed in *Scn1a*$^{+/-}$ mice compared to WT at P13-14 (Fig. 6F), a feature
15 that has been related to slowed and abnormal development of neuronal networks, also linked to
16 anomalies in the development of the GABAergic system (53, 54). Thus, we recorded GABAergic
17 (sIPSCs) and glutamatergic (sEPSCs) post-synaptic currents in pyramidal cells of the CA1-area of
18 hippocampal slices obtained from P11-12 *Scn1a*$^{+/-}$ mice (Fig.7A). We found a clear reduction in
19 frequency (Fig.7C) and a mild reduction in amplitude of sIPSCs (Fig.7E) already at this early stage of
20 development. Moreover, we observed a mild reduction in the amplitude of sEPSCs, although their
21 frequency was not modified (Fig. 2F).

22 GABA has trophic actions on dendritic processes and synapse formation during early development
23 (55–58), and reduced release of depolarizing GABA may cause a delay in maturation. Moreover,
24 KCC2, which we found downregulated in *Scn1a*$^{+/-}$ mice, is implicated in spine formation and
25 maturation (57). We evaluated the features of dendritic spines of pyramidal neurons in the CA1 area
26 of the hippocampus by using Golgi staining (Fig.8 A-B) and indeed observed a decreased spine head
27 width at both P11 and P21 in *Scn1a*$^{+/-}$ mice (Fig.8C), whereas spine density was not modified (Fig.8D).
28 This is consistent with an impairment of dendritic spine maturation.

29 Taken together these data show a neurodevelopmental component in *Scn1a*$^{+/-}$ DS mice, with
30 alterations appearing at early developmental stages before the onset of seizures, in which the
31 decreased release of GABA and the consequences on its trophic actions may be involved.

32

# Discussion

The disease onset in DEEs is often considered as the onset of seizures, which is the initial most evident symptom of the pathology, but other dysfunctions, in particular cognitive/behavioral ones, may begin to develop earlier, and they are a persistent major burden in DS. Although numerous studies have reported in DS mouse models hypoexcitability of GABAergic neurons and reduced GABAergic synaptic transmission in the period preceding the onset of spontaneous seizures (11–15, 18, 59), little is known about the link between these early dysfunctions of neuronal networks and the development of cognitive/behavioral defects. In particular, early pre-epileptic dysfunctions in the GABAergic system may lead to neurodevelopmental delay and contribute to the generation of neuropsychiatric symptoms (30, 58, 60). Interestingly, a delayed GABA-switch has been reported in models of DS (24, 27). However, its importance as a pathological mechanism in DS has not been investigated yet, although a study showed that its pharmacological rescue with bumetanide was able to delay mortality in the *Scn1b*$^{-/-}$ mouse model of sodium channel β1 subunit DEE (24), which is a different clinical entity than DS (1, 25, 26).

Here we assessed the importance of the delay in the GABA-switch as a pathological mechanism in *Scn1a*$^{+/-}$ mice, rescuing it by targeting either KCC2 or NKCC1 with KU55933 (KU) or bumetanide, respectively, and evaluating the effect on both epileptic and cognitive/behavioral features. For increasing the translational value of the results, we started the treatments at P15, an age that should correspond to the onset of the febrile stage in patients. Both drugs rescued social interaction deficits observed in P21 *Scn1a*$^{+/-}$ mice and ameliorated hyperactivity in the Y maze test; bumetanide improved also spatial working memory deficits. Although its blood-brain barrier permeability is low, similar bumetanide treatments have been effectively used in several *in vivo* studies of mouse models of neurodevelopmental diseases (43–45). In particular, our results are in agreement with previous studies showing beneficial effects of bumetanide treatment on hyperactivity in mice with dysfunctional $K_V7$ voltage-gated $K^+$ channels (61) and on both hyperactivity and social behavior in patients with tuberous sclerosis complex (TSC) (62). Thus, bumetanide, as well as other drugs targeting GABA-switch that may be approved in the future for clinical use (possibly including KU), could be beneficial also for DS patients. Taken together, our data suggest that GABA-switch delay is implicated in neuropsychiatric comorbidities of DS, in particular sociability defects, a prominent feature of ASD. Conversely, neither KU nor bumetanide ameliorated the epileptic phenotype (hyperthermia-induced seizures, spontaneous seizures or mortality), although alterations of GABA-switch and KCC2 expression level/activity have been identified in epilepsy (63) and in our *ex vivo*

experiments the KU treatment also decreased the frequency of spontaneous excitatory events in *Scn1a*$^{+/-}$ mice . This may be linked to the lack of effect of the treatment that we used on the reduced GABAergic synaptic transmission of *Scn1a*$^{+/-}$ mice, which characterizes DS models and that is thought to be implicated in DS epileptogenesis.

Importantly, in addition to the delayed GABA-switch, we demonstrated that DS mice display behavioral defects and delayed neurodevelopmental milestones at very early stages before seizure onset, including olfactory discrimination deficits of nest bedding, which we observed at P10, and delayed eye opening. This is consistent with an early effect of the *Scn1a* mutation. In fact, we have shown that DS mice display a reduction of spontaneous GABAergic synaptic currents in CA1 pyramidal hippocampal neurons already at P11-12, an early developmental stage (well before seizure onset) at the beginning of $Na_V1.1$ expression, which in mice is at around P8 (16). As already proposed in numerous previous studies (11, 12, 14, 64), the reduced frequency of sIPSCs can directly depend on the $Na_V1.1$ loss-of-function induced by DS mutations, which leads to a reduction of sodium current and excitability of GABAergic interneurons. However, this initial dysfunction of the GABAergic system could induce also a more general maturation delay. In fact, GABA exerts a trophic action at early stages of neurodevelopment promoting cell survival differentiation and migration, expression of brain-derived neurotrophic factor (BDNF), and spine maturation (55, 57, 65). Notably, GABA itself can promote GABA-switch (66) and reduced GABAergic transmission in *Scn1a*$^{+/-}$ mice may interfere with it. Thus, because of its trophic role in neurodevelopment, the decreased GABA release in *Scn1a*$^{+/-}$ mice might be implicated in the behavioral defects, reduced amplitude of sEPSCs, and modifications of spine morphology that we have observed already at early developmental stages (P11-12). Our functional data correlated with the results of our western blot experiments, which showed decreased expression of KCC2 in the hippocampus of *Scn1a*$^{+/-}$ mice. This is at odds with the results reported for another Scn1a$^{+/-}$ model that showed no modification of KCC2 expression, although a delay in GABA-switch was observed (24). However, that study used total brain membranes for western blot and a mixed 129×C57BL/6J genetic background that gives milder cellular dysfunctions and phenotype compared to the pure C57BL/6J mice that we used (12, 67), which may explain the different results.

Interestingly, KCC2, independently of its chloride transport function, plays an important role in the development and morphology of dendritic spines through interaction with post-synaptic proteins and signalling pathways, leading to a remodelling of the spine's actin cytoskeleton (32). This function could be implicated in the reduced spine head size without reduction of spine density that we

observed in *Scn1a*$^{+/-}$ mice. Consistently, KCC2 knock-out mice display spines with immature morphology (no obvious spine heads), whereas the density of the dendritic protrusions is not affected (68). Thin filopodia-like spine heads are considered less mature, indicating early stages of synapse formation or a lack of synaptic stabilization. Notably, altered spine morphology, including reduced head width, has been associated with pathological conditions, in particular neurodevelopmental diseases (69). Also other dysfunctions that we have observed in *Scn1a*$^{+/-}$ mice (i.e. E/I imbalance, defective GABAergic transmission, delay in neurodevelopmental milestones such as eye opening and GABA-switch) are key features observed in animal models of neurodevelopmental disorders, for example Down syndrome, Rett syndrome, Fragile X syndrome and the VPA model of autism spectrum disorder (31, 36, 70–72).

Our data showing the effects on behavioral dysfunctions, but not on seizures, of treatments targeting the delayed GABA-switch, as well as those showing early neurodevelopmental defects before seizure onset, demonstrate that DS mice display a neurodevelopmental delay that is specifically linked to the cognitive/behavioral phenotype, but not the epileptic phenotype. Thus, we disclose a neurodevelopmental component in DS which selectively impacts the behavioral phenotype, in particular autistic-like traits. We provide here new experimental evidence to the hypothesis that cognitive/behavioral defects in DS can develop before the onset of spontaneous seizures, as observed for some motor features and hyperactivity in the Scn1a$^{A1783V/+}$ knock-in mouse model (73), and that they can be uncoupled from seizures and have specific pathological mechanisms, at least at the early stages of the disease. This can be relevant in a translational perspective. In fact, DS treatments are currently started after seizure onset and are mainly targeted to alleviation of seizures, whereas there are still no effective treatments against the cognitive/behavioral comorbidities, which are among the most severe phenotypic features, especially at later stages of the disease. Our results suggest novel therapeutic options for DS that can target cognitive/behavioral defects separately from seizures with specific pharmacological interventions that should be started as early as possible. In particular, targeting the GABA-switch may be an innovative pharmacological strategy to ameliorate DS behavioral defects.

Overall, our results are consistent with partially specific pathological mechanisms for seizures and some cognitive/behavioural defects in DS. The early reduction of GABA release in DS could determine a cascade of events resulting in an abnormal neurodevelopmental trajectory, including delayed GABA-switch, because of the trophic role of GABA in neurodevelopment. These dysfunctions may be specifically targeted in therapy.

# Material and methods

See Supplementary Material for details.

**Animals.**

F1 mice used for the experiments were generated mating floxed homozygous *Scn1a* C57BL/6J females (15, 48) and heterozygote Meox2-Cre C57BL/6J males (Jackson Laboratories, stock No: 003755) to obtain *Scn1a*$^{+/-}$ mice. Animal experimental protocols have been validated by ethics committees (CIEPAL Azur) and the French Ministry of research under the agreement number APAFIS#9901-2017040616024590v6-PEA216/408 and APAFIS#15665-201805301624157v2-PEA499.

**Pharmacological treatments.**

KU55933 (Tocris, S1092) was delivered with intranasal administrations, Bumetanide (Sigma, B3023) with intraperitoneal injections.

**Brain slice preparation and electrophysiological recordings.**

We prepared brain slices from mice deeply anesthetized with Isoflurane and performed patch clamp recordings in whole cell and loose patch configurations as in (74, 75).

**Golgi staining.**

WT and *Scn1a*$^{+/-}$ mice (males and females; P11 or P21) were deeply anesthetized with intra-peritoneal injections of Kétamine and Xylasine, and intracardiacally perfused with saline (0,9% NaCl) to remove blood followed by 4% paraformaldehyde. Golgi-Cox staining was performed as in (76, 77).

**Western Blotting.**

Proteins were obtained from explanted hippocampus, homogenized in sample buffer separated by SDS-PAGE electrophoresis, blotted, and incubated with primary antibody followed by HRP-conjugated secondary antibody, as in (36).

**Behavioral tests.**

The tests for evaluating early neurodevelopmental maturation (righting reflex, forepaw grasping reflex, negative geotaxis reflex, gait, nest-bedding/homing and eye opening) were performed from P7 to P14 as described in the Supplementary Material. For these experiments, we also compared heterozygote Meox2-Cre mice with WT littermates and observed no differences (Supplementary Fig. 2). Other behavioral tests (three-chamber test, Y maze) were performed at P21-22 as described in the Supplementary Material.

**Seizure induction by hyperthermia and video analysis of spontaneous seizures**

Seizures were induced by hyperthermia and their severity were quantified with a modified Racine scale as previously described (78). Spontaneous convulsive seizures were quantified analyzing continuous video recordings with a software program (SASDI) that we developed (46).

**Data analysis and statistics.**

Data analysis and statistical tests were performed with the following softwares: pClamp 10 (Molecular Devices, USA), Excel (Microsoft Office), ImageJ, Prism9 (GraphPad Software) and OriginPro2021 (OriginLab). Statistical tests were performed using the appropriate parametric or non-parametric statistical test, according to the type of data and comparison (see Supplementary Material). Differences were considered significant when P values where smaller than 0.05.

# Acknowledgments

We thank Emilie Bonnet (Institute of Molecular and Cellular Pharmacology, CNRS UMR 7275 and University Cote d'Azur) for her skillful technical support. This work was funded by UCAJEDI (https://univ-cotedazur.fr/ucajedi-lidex-duniversite-cote-dazur, ANR-15-IDEX-01, France), Laboratory of Excellence "Ion Channel Science and Therapeutics" - LabEx ICST (https://www.labex-icst.fr/en, ANR-11-LABX-0015-01, France) and EJPRD *SCN1A*-UP! (ANR-20-RAR4-0001, France) to MM. LP received a postdoc fellowship from the Fondazione Umberto Veronesi, Italy. FA was supported by Italian Ministry of University and Research, PRIN: Progetti di ricerca di rilevanza nazionale, 2022 (https://prin.mur.gov.it/Pages/Index/119) Prot.20229XWM5L, and PRIN: Progetti di ricercar di rilevanza nazionale, 2017 Prot. 20175C22WM.

# References

1. Guerrini R, et al. Developmental and epileptic encephalopathies: from genetic heterogeneity to phenotypic continuum. *Physiological Reviews*. 2023;103(1):433–513.

2. Dravet C, et al. Severe myoclonic epilepsy in infancy: Dravet syndrome. *Adv Neurol*. 2005;95:71–102.

3. Wirrell EC, et al. International consensus on diagnosis and management of Dravet syndrome. *Epilepsia*. 2022;63(7):1761–1777.

4. Claes L, et al. De novo mutations in the sodium-channel gene SCN1A cause severe myoclonic epilepsy of infancy. *Am J Hum Genet*. 2001;68(6):1327–1332.

5. Gataullina S, Dulac O. From genotype to phenotype in Dravet disease. *Seizure - European Journal of Epilepsy*. 2017;44:58–64.

6. Li B-M, et al. Autism in Dravet syndrome: Prevalence, features, and relationship to the clinical characteristics of epilepsy and mental retardation. *Epilepsy & Behavior*. 2011;21(3):291–295.

7. Brunklaus A, et al. Prognostic, clinical and demographic features in SCN1A mutation-positive Dravet syndrome. *Brain*. 2012;135(Pt 8):2329–2336.

8. Sinoo C, et al. Behavior problems and health-related quality of life in Dravet syndrome. *Epilepsy & Behavior*. 2019;90:217–227.

9. Ouss L, et al. Autism spectrum disorder and cognitive profile in children with Dravet syndrome: Delineation of a specific phenotype. *Epilepsia Open*. 2019;4(1):40–53.

10. Wirrell EC. Treatment of Dravet Syndrome. *Canadian Journal of Neurological Sciences*. 2016;43(S3):S13–S18.

11. Han S, et al. Autistic-like behaviour in Scn1a+/− mice and rescue by enhanced GABA-mediated neurotransmission. *Nature*. 2012;489(7416):385–390.

12. Yu FH, et al. Reduced sodium current in GABAergic interneurons in a mouse model of severe myoclonic epilepsy in infancy. *Nat Neurosci*. 2006;9(9):1142–1149.

13. Mantegazza M, Cestèle S, Catterall WA. Sodium channelopathies of skeletal muscle and brain. *Physiological Reviews*. 2021;101(4):1633–1689.

14. Mantegazza M, Broccoli V. SCN1A/NaV1.1 channelopathies: Mechanisms in expression systems, animal models, and human iPSC models. *Epilepsia*. 2019;60(S3):S25–S38.

15. Cheah CS, et al. Specific deletion of $Na_V$ 1.1 sodium channels in inhibitory interneurons causes seizures and premature death in a mouse model of Dravet syndrome. *Proc Natl Acad Sci USA*. 2012;109(36):14646–14651.

16. Ogiwara I, et al. Nav1.1 Localizes to Axons of Parvalbumin-Positive Inhibitory Interneurons: A Circuit Basis for Epileptic Seizures in Mice Carrying an Scn1a Gene Mutation. *Journal of Neuroscience*. 2007;27(22):5903–5914.

17. Stern WM, et al. Impaired intracortical inhibition demonstrated in vivo in people with Dravet syndrome. *Neurology*. 2017;88(17):1659–1665.

18. Kaneko K, et al. Developmentally regulated impairment of parvalbumin interneuron synaptic transmission in an experimental model of Dravet syndrome. *Cell Reports*. 2022;38(13):110580.

19. Riva D, et al. Progressive neurocognitive decline in two children with Dravet syndrome, de novo SCN1A truncations and different epileptic phenotypes. *Am J Med Genet A*. 2009;149A(10):2339–2345.

20. Guzzetta F. Cognitive and behavioral characteristics of children with Dravet syndrome: an overview. *Epilepsia*. 2011;52 Suppl 2:35–38.

21. Catarino CB, et al. Dravet syndrome as epileptic encephalopathy: evidence from long-term course and neuropathology. *Brain*. 2011;134(Pt 10):2982–3010.

22. Nabbout R, et al. Encephalopathy in children with Dravet syndrome is not a pure consequence of epilepsy. *Orphanet Journal of Rare Diseases*. 2013;8(1):176.

23. Li W, Schneider AL, Scheffer IE. Defining Dravet syndrome: An essential pre-requisite for precision medicine trials. *Epilepsia*. 2021;62(9):2205–2217.

24. Yuan Y, et al. Delayed maturation of GABAergic signaling in the Scn1a and Scn1b mouse models of Dravet Syndrome. *Sci Rep*. 2019;9(1):6210.

25. Aeby A, et al. SCN1B-linked early infantile developmental and epileptic encephalopathy. *Annals of Clinical and Translational Neurology*. 2019;6(12):2354–2367.

26. Scala M, et al. Homozygous SCN1B variants causing early infantile epileptic encephalopathy 52 affect voltage-gated sodium channel function. *Epilepsia*. 2021;62(6):e82–e87.

27. Ruffolo G, et al. A novel GABAergic dysfunction in human Dravet syndrome. *Epilepsia*. 2018;59(11):2106–2117.

28. Watanabe M, Fukuda A. Development and regulation of chloride homeostasis in the central nervous system. *Front Cell Neurosci*. 2015;9. https://doi.org/10.3389/fncel.2015.00371.

29. Owens DF, Kriegstein AR. Is there more to gaba than synaptic inhibition? *Nat Rev Neurosci*. 2002;3(9):715–727.

30. Ben-Ari Y. Excitatory actions of gaba during development: the nature of the nurture. *Nat Rev Neurosci*. 2002;3(9):728–739.

31. Deidda G, Bozarth IF, Cancedda L. Modulation of GABAergic transmission in development and neurodevelopmental disorders: investigating physiology and pathology to gain therapeutic perspectives. *Frontiers in Cellular Neuroscience*. 2014;8. https://www.frontiersin.org/article/10.3389/fncel.2014.00119. Accessed June 17, 2022.

1 32. Kaila K, et al. Cation-chloride cotransporters in neuronal development, plasticity and disease. *Nat Rev*
2 *Neurosci*. 2014;15(10):637–654.

3 33. Khazipov R, Valeeva G, Khalilov I. Depolarizing GABA and Developmental Epilepsies. *CNS Neuroscience &*
4 *Therapeutics*. 2015;21(2):83–91.

5 34. Tyzio R, et al. Oxytocin-Mediated GABA Inhibition During Delivery Attenuates Autism Pathogenesis in
6 Rodent Offspring. *Science*. 2014;343(6171):675–679.

7 35. Schulte JT, Wierenga CJ, Bruining H. Chloride transporters and GABA polarity in developmental,
8 neurological and psychiatric conditions. *Neuroscience & Biobehavioral Reviews*. 2018;90:260–271.

9 36. Pizzamiglio L, et al. The DNA repair protein ATM as a target in autism spectrum disorder. *JCI*
10 *Insight*;6(3):e133654.

11 37. Focchi E, et al. ATM rules neurodevelopment and glutamatergic transmission in the hippocampus but
12 not in the cortex. *Cell Death Dis*. 2022;13(7):616.

13 38. Ward OC, Lam LK. Bumetanide in heart failure in infancy. *Arch Dis Child*. 1977;52(11):877–882.

14 39. Lemonnier E, et al. A randomised controlled trial of bumetanide in the treatment of autism in children.
15 *Transl Psychiatry*. 2012;2(12):e202–e202.

16 40. Fernell E, Gustafsson P, Gillberg C. Bumetanide for autism: Open-label trial in six children. *Acta*
17 *Paediatr*. 2021;110(5):1548–1553.

18 41. Liautard C, et al. Hippocampal hyperexcitability and specific epileptiform activity in a mouse model of
19 Dravet syndrome. *Epilepsia*. 2013;54(7):1251–1261.

20 42. Jansen NA, et al. Focal and generalized seizure activity after local hippocampal or cortical ablation of
21 NaV 1.1 channels in mice. *Epilepsia*. 2020;61(4):e30–e36.

43. Deidda G, et al. Reversing excitatory GABAAR signaling restores synaptic plasticity and memory in a mouse model of Down syndrome. *Nat Med*. 2015;21(4):318–326.

44. Sivakumaran S, Maguire J. Bumetanide reduces seizure progression and the development of pharmacoresistant status epilepticus. *Epilepsia*. 2016;57(2):222–232.

45. Dargaei Z, et al. Restoring GABAergic inhibition rescues memory deficits in a Huntington's disease mouse model. *Proc Natl Acad Sci U S A*. 2018;115(7):E1618–E1626.

46. Diaz-Arce D, et al. A python-based package for long-lasting video acquisition and semi-automated detection of convulsive seizures in rodents [preprint]. 2022;2022.04.15.488472.

47. Ito S, et al. Mouse with Nav1.1 haploinsufficiency, a model for Dravet syndrome, exhibits lowered sociability and learning impairment. *Neurobiology of Disease*. 2013;49:29–40.

48. Williams AD, et al. A more efficient conditional mouse model of Dravet syndrome: Implications for epigenetic selection and sex-dependent behaviors. *Journal of Neuroscience Methods*. 2019;325:108315.

49. Rubinstein M, et al. Dissecting the phenotypes of Dravet syndrome by gene deletion. *Brain*. 2015;138(Pt 8):2219–2233.

50. Roullet FI, et al. Behavioral and molecular changes in the mouse in response to prenatal exposure to the anti-epileptic drug valproic acid. *Neuroscience*. 2010;170(2):514–522.

51. Moldrich RX, et al. Inhibition of histone deacetylase in utero causes sociability deficits in postnatal mice. *Behavioural Brain Research*. 2013;257:253–264.

52. Cinque C, et al. Modeling socially anhedonic syndromes: genetic and pharmacological manipulation of opioid neurotransmission in mice. *Transl Psychiatry*. 2012;2(8):e155–e155.

53. Chattopadhyaya B, et al. Experience and Activity-Dependent Maturation of Perisomatic GABAergic Innervation in Primary Visual Cortex during a Postnatal Critical Period. *J Neurosci*. 2004;24(43):9598–9611.

54. Guan W, et al. Eye opening differentially modulates inhibitory synaptic transmission in the developing visual cortex. *eLife*. 2017;6:e32337.

55. Cancedda L, et al. Excitatory GABA Action Is Essential for Morphological Maturation of Cortical Neurons In Vivo. *J Neurosci*. 2007;27(19):5224–5235.

56. Wang DD, Kriegstein AR. Blocking Early GABA Depolarization with Bumetanide Results in Permanent Alterations in Cortical Circuits and Sensorimotor Gating Deficits. *Cerebral Cortex*. 2011;21(3):574–587.

57. Awad PN, et al. KCC2 Regulates Dendritic Spine Formation in a Brain-Region Specific and BDNF Dependent Manner. *Cerebral Cortex*. 2018;28(11):4049–4062.

58. Peerboom C, Wierenga CJ. The postnatal GABA shift: A developmental perspective. *Neuroscience & Biobehavioral Reviews*. 2021;124:179–192.

59. Almog Y, et al. Developmental alterations in firing properties of hippocampal CA1 inhibitory and excitatory neurons in a mouse model of Dravet syndrome. *Neurobiology of Disease*. 2021;148:105209.

60. Tang X, Jaenisch R, Sur M. The role of GABAergic signalling in neurodevelopmental disorders. *Nat Rev Neurosci*. 2021;22(5):290–307.

61. Marguet SL, et al. Treatment during a vulnerable developmental period rescues a genetic epilepsy. *Nat Med*. 2015;21(12):1436–1444.

62. van Andel DM, et al. Effects of bumetanide on neurodevelopmental impairments in patients with tuberous sclerosis complex: an open-label pilot study. *Mol Autism*. 2020;11(1):30.

63. Di Cristo G, et al. KCC2, epileptiform synchronization, and epileptic disorders. *Progress in Neurobiology*. 2018;162:1–16.

64. Almog Y, et al. Developmental alterations in firing properties of hippocampal CA1 inhibitory and excitatory neurons in a mouse model of Dravet syndrome. *Neurobiology of Disease*. 2021;148:105209.

1 65. Obrietan K, Gao X-B, van den Pol AN. Excitatory Actions of GABA Increase BDNF Expression via a MAPK-
2 CREB–Dependent Mechanism—A Positive Feedback Circuit in Developing Neurons. *Journal of*
3 *Neurophysiology*. 2002;88(2):1005–1015.

4 66. Ganguly K, et al. GABA Itself Promotes the Developmental Switch of Neuronal GABAergic Responses
5 from Excitation to Inhibition. *Cell*. 2001;105(4):521–532.

6 67. Rubinstein M, et al. Genetic background modulates impaired excitability of inhibitory neurons in a
7 mouse model of Dravet syndrome. *Neurobiology of Disease*. 2015;73:106–117.

8 68. Li H, et al. KCC2 Interacts with the Dendritic Cytoskeleton to Promote Spine Development. *Neuron*.
9 2007;56(6):1019–1033.

10 69. Martínez-Cerdeño V. Dendrite and spine modifications in autism and related neurodevelopmental
11 disorders in patients and animal models. *Developmental Neurobiology*. 2017;77(4):393–404.

12 70. Chao H-T, et al. Dysfunction in GABA signalling mediates autism-like stereotypies and Rett syndrome
13 phenotypes. *Nature*. 2010;468(7321):263–269.

14 71. Lozovaya N, et al. Early alterations in a mouse model of Rett syndrome: the GABA developmental shift
15 is abolished at birth. *Sci Rep*. 2019;9(1):9276.

16 72. He Q, et al. The Developmental Switch in GABA Polarity Is Delayed in Fragile X Mice. *J Neurosci*.
17 2014;34(2):446–450.

18 73. Fadila S, et al. Convulsive seizures and some behavioral comorbidities are uncoupled in the
19 Scn1aA1783V Dravet syndrome mouse model. *Epilepsia*. 2020;61(10):2289–2300.

20 74. Chever O, et al. Initiation of migraine-related cortical spreading depolarization by hyperactivity of
21 GABAergic neurons and NaV1.1 channels. *J Clin Invest*;131(21):e142203.

1 75. Lemaire L, et al. Modeling NaV1.1/SCN1A sodium channel mutations in a microcircuit with realistic ion
2 concentration dynamics suggests differential GABAergic mechanisms leading to hyperexcitability in
3 epilepsy and hemiplegic migraine. *PLoS Comput Biol*. 2021;17(7):e1009239.

4 76. Menna E, et al. Eps8 controls dendritic spine density and synaptic plasticity through its actin-capping
5 activity. *EMBO J*. 2013;32(12):1730–1744.

6 77. Bayram-Weston Z, et al. Optimising Golgi-Cox staining for use with perfusion-fixed brain tissue
7 validated in the zQ175 mouse model of Huntington's disease. *J Neurosci Methods*. 2016;265:81–88.

8 78. Salgueiro-Pereira AR, et al. A two-hit story: Seizures and genetic mutation interaction sets phenotype
9 severity in SCN1A epilepsies. *Neurobiology of Disease*. 2019;125:31–44.

10
11

# Figures

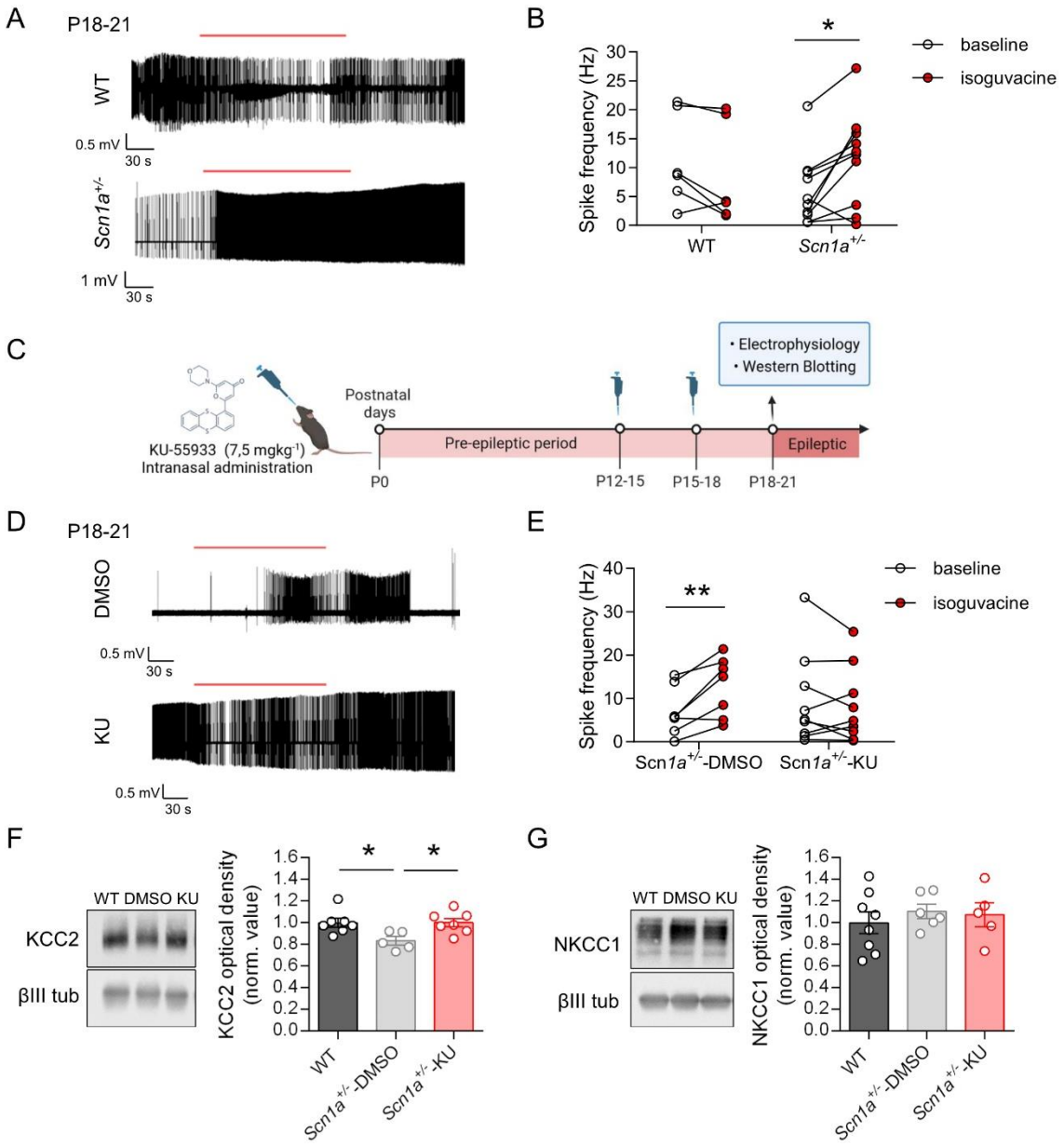


**Figure 1. KU rescues the altered GABA switch in *Scn1a*$^{+/-}$ mice.**

**A.** Representative traces of CA3 pyramidal cells' spontaneous spiking activity measured by current clamp (I=0) recordings in loose patch configuration. Cells were recorded for 3/5 minutes to obtain a stable control baseline, isoguvacine (10 µM) was bath applied for 3 minutes (bars above the traces) and washed out for at least 10 minutes. **B.** Analysis of mean spike frequency in control and upon isoguvacine application in WT (n = 6 cells, N = 3 mice) or *Scn1a*$^{+/-}$ (n = 10 cells, N = 3 mice) CA3 pyramidal neurons revealed an excitatory effect of the GABA agonist in *Scn1a*$^{+/-}$ mice whereas no difference between control and isoguvacine were observed in WT (WT baseline: mean ± SEM = 11.29 ± 3.25; WT isoguvacine: mean ± SEM = 8.57 ± 3.56; *Scn1a*$^{+/-}$ baseline: mean ± SEM = 6.09 ±

1.94; *Scn1a*$^{+/-}$ isoguvacine: mean ± SEM = 11.52 ± 2.58). Paired t test, p-value: WT = 0.0702, *Scn1a*$^{+/-}$ = 0.0129. **C.** Schematic representation of KU55933 (KU) treatment and experimental timeline. For comparing littermates in *ex-vivo* electrophysiological recordings, we used sliding windows: mice received two intranasal administrations (every 72 hours) of KU or vehicle (DMSO), the first in the window P12-P15 and the second in the window P15-18, and recordings were performed in the window P18-P21. For western blotting analysis, mice received two intranasal administrations (every 72 hours) at 15 and P18, and western blot was performed at P21. **D.** Representative traces of P18-21 CA3 pyramidal cells' spiking activity and effect of isoguvacine (10 µM; bar above the traces) measured in A. **E.** Analysis of mean spike frequency of baseline and upon isoguvacine application (bars above the traces) of *Scn1a*$^{+/-}$-DMSO (n=7 cells, N = 3 mice) and *Scn1a*$^{+/-}$-KU (n=9 cells, N = 4 mice) CA3 pyramidal neurons revealed an excitatory effect of GABA in vehicle-treated *Scn1a*$^{+/-}$ mice, whereas no modification between baseline and isoguvacine was found in KU-treated animals (DMSO baseline: mean ± SEM = 6.97 ± 2.13; DMSO isoguvacine: mean ± SEM = 12.69 ± 2.62; KU baseline: mean ± SEM = 9.51 ± 3.56; KU isoguvacine: mean ± SEM = 8.32 ± 2.89). Paired t-test, p-value: DMSO = 0.009, KU = 0.405. **F.** Western blotting quantification of P21 hippocampal tissues showed a reduced expression of KCC2 chloride transporter in *Scn1a*$^{+/-}$ mice, which is related to GABA switch delay. KU treatment rescued this alteration increasing KCC2 expression (WT: mean ± SEM = 1.000 ± 0.041, N = 7; Scn1a$^{+/-}$-DMSO: mean ± SEM = 0.833 ± 0.038, N = 5; Scn1a$^{+/-}$-KU: mean ± SEM = 1.001 ± 0.037, N = 7; values normalized to the mean of the WT). One-Way ANOVA, Fisher's LSD post-hoc test, p-value: WT vs Scn1a$^{+/-}$-DMSO = 0.0111, WT vs. Scn1a$^{+/-}$-KU = 0.9789, Scn1a$^{+/-}$-DMSO vs. Scn1a$^{+/-}$-KU = 0.0106. **G.** There was no difference in NKCC2 levels in the three conditions (WT: mean ± SEM = 1.000 ± 0.098, N = 8; Scn1a$^{+/-}$- DMSO: mean ± SEM = 1.104 ± 0.065, N = 6; Scn1a$^{+/-}$-KU: mean ± SEM = 1.073 ± 0.117; N = 5). One-Way ANOVA, Fisher's LSD post-hoc test, p-value: WT vs Scn1a$^{+/-}$-DMSO = 0.4321, WT vs. Scn1a$^{+/-}$-KU = 0.5982, Scn1a$^{+/-}$-DMSO vs. Scn1a$^{+/-}$-KU = 0.8344.

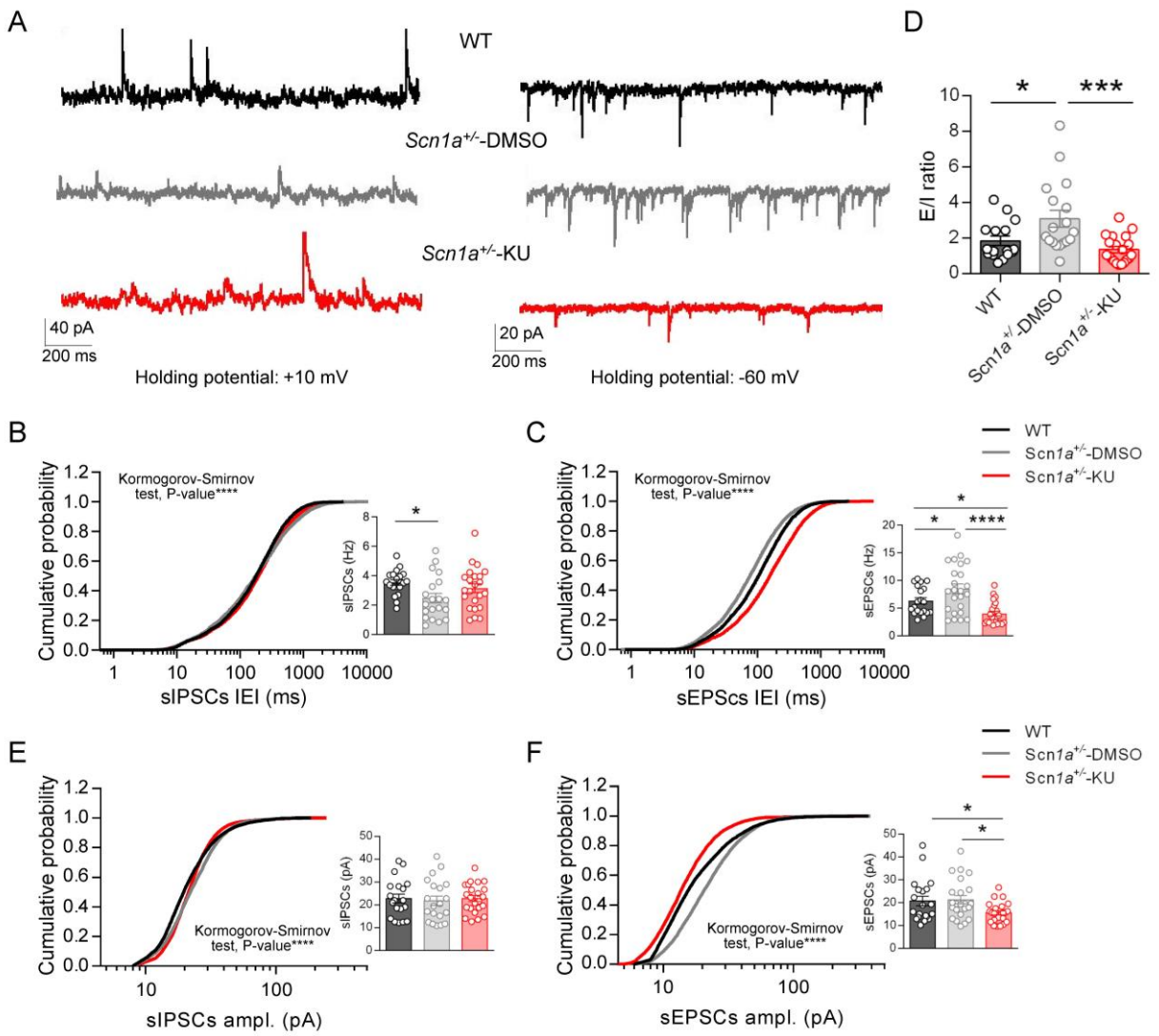


**Figure 2. KU ex-vivo characterizationin P18-21 *Scn1a*$^{+/-}$ mice: effect on spontaneous synaptic activity.**

**A.** Representative traces of spontaneous GABAergic post-synaptic currents (sIPSCs) and spontaneous glutamatergic post-synaptic currents (sEPSCs) recorded at +10 mV and -60 mV, respectively, in pyramidal neurons from hippocampal CA1 slices of vehicle-treated (DMSO) or KU-treated *Scn1a*$^{+/-}$ mice compared to WT littermates. **B.** The cumulative distribution showed an increased inter-event interval (IEI) of sIPSCs in vehicle-treated *Scn1a*$^{+/-}$ mice compared to WT. KU treatment decreased sIPSCs IEI in *Scn1a*$^{+/-}$ treated animals (WT: n = 19 cells, N = 6 animals; Scn1a$^{+/-}$ - DMSO: n = 20 cells, N = 8 animals; *Scn1a*$^{+/-}$- KU: n = 23 cells, N = 6 animals, KS test p-value <0.0001). Consistently, the comparison of mean sIPSCs frequency showed a decrease in vehicle-treated *Scn1a*$^{+/-}$ mice compared to WT, which was partially rescued in KU-treated *Scn1a*$^{+/-}$ mice (WT: mean ± SEM = 3.54 ± 0.19, n = 19 cells, N = 6 animals; *Scn1a*$^{+/-}$- DMSO mean ± SEM = 2.48 ± 0.33, n = 20 cells, N = 8 animals; *Scn1a*$^{+/-}$- KU: mean ± SEM = 3.15 ± 0.29, n = 23 cells, N = 6 animals). One-Way

ANOVA, Fisher's LSD post-hoc test, p-value: WT vs Scn1a$^{+/-}$-DMSO = 0.0130, WT vs. Scn1a$^{+/-}$-KU = 0.3270, Scn1a$^{+/-}$-DMSO vs. Scn1a$^{+/-}$-KU = 0.0978. **C.** The cumulative distribution of sEPSCs IEIs displayed a decrease in vehicle-treated *Scn1a*$^{+/-}$ mice and KU treatment rescued this defect but increasing the IEI above WT level (WT: n = 20 cells, N = 6 animals; Scn1a$^{+/-}$- DMSO: n = 24 cells, N = 8 animals; Scn1a$^{+/-}$- KU: n = 24 cells, N = 6 animals, KS test p-value <0.0001). Consistently, the comparison of mean sEPSCs frequency showed an increase in *Scn1a*$^{+/-}$ compared to WT and KU administration rescued this defect, but reducing the mean sEPSCs frequency below that of WT (WT: mean ± SEM = 6.30 ± 0.56, n = 20 cells, N = 6 animals; *Scn1a*$^{+/-}$- DMSO: mean ± SEM = 8.45 ± 0.89, n = 24 cells, N = 8 animals; *Scn1a*$^{+/-}$- KU: mean ± SEM = 3.99 ± 0.41, n = 24 cells, N = 6 animals). One-Way ANOVA, Fisher's LSD post-hoc test, p-value: WT vs Scn1a$^{+/-}$-DMSO = 0.0286, WT vs. Scn1a$^{+/-}$-KU = 0.0190, Scn1a$^{+/-}$-DMSO vs. Scn1a$^{+/-}$-KU <0.0001. **D.** The excitatory/inhibitory ratio (E/I) was obtained dividing mean sEPSCs and sIPSCs frequencies measured of the same neuron (WT: mean ± SEM = 1.85 ± 0.26, n = 16 cells, N = 6 animals; *Scn1a*$^{+/-}$- DMSO: mean ± SEM = 3.09 ± 0.47, n = 18 cells, N = 8 animals; *Scn1a*$^{+/-}$- KU: mean ± SEM = 1.36 ± 0.17, n = 20 cells, N = 6 animals). One-Way ANOVA, Fisher's LSD post-hoc test, p-value: WT vs Scn1a$^{+/-}$-DMSO = 0.0108, WT vs. Scn1a$^{+/-}$-KU = 0.2951, Scn1a$^{+/-}$-DMSO vs. Scn1a$^{+/-}$-KU = 0.0003. **E.** The cumulative distribution of sIPSCs amplitude showed a slight difference between the distributions (KS test p-value <0.0001), which did not reach statistical significance comparing mean values (WT: mean ± SEM = 22.85 ± 1.957, n = 19 cells, N = 6 animals; *Scn1a*$^{+/-}$- DMSO mean ± SEM = 21.87 ± 2.062, n = 20 cells, N = 8 animals; *Scn1a*$^{+/-}$- KU: mean ± SEM = 22.86 ± 1.325, n = 23 cells, N = 6 animals). One-Way ANOVA, Fisher's LSD post-hoc test, p-value: WT vs Scn1a$^{+/-}$-DMSO = 0.7050, WT vs. Scn1a$^{+/-}$-KU = 0.9962, Scn1a$^{+/-}$-DMSO vs. Scn1a$^{+/-}$-KU = 0.6881. **F.** The cumulative distribution of sEPSCs amplitudes showed an increase in vehicle-treated *Scn1a*$^{+/-}$ mice (n = 23, N = 8 animals) and a decrease in KU-treated ones (n = 24, N = 6 animals) compared to WT (n = 20, N = 6 animals), KS test p-value <0.0001. The decrease in vehicle-treated *Scn1a*$^{+/-}$ mice was not observed comparing mean values, whereas KU treatment decreased sEPSCs amplitude below WT level also considering mean values (WT: mean ± SEM = 20.79 ± 2.101; *Scn1a*$^{+/-}$ - DMSO: mean ± SEM = 21.37 ± 1.804; *Scn1a*$^{+/-}$-KU: mean ± SEM = 15.57 ± 0.8966), One-Way ANOVA, Fisher's LSD post-hoc test. P<0.0001; One-Way ANOVA, Fisher's LSD post-hoc test, p-value: WT vs Scn1a$^{+/-}$-DMSO = 0.8057, WT vs. Scn1a$^{+/-}$-KU = 0.0281, Scn1a$^{+/-}$-DMSO vs. Scn1a$^{+/-}$-KU = 0.0119.

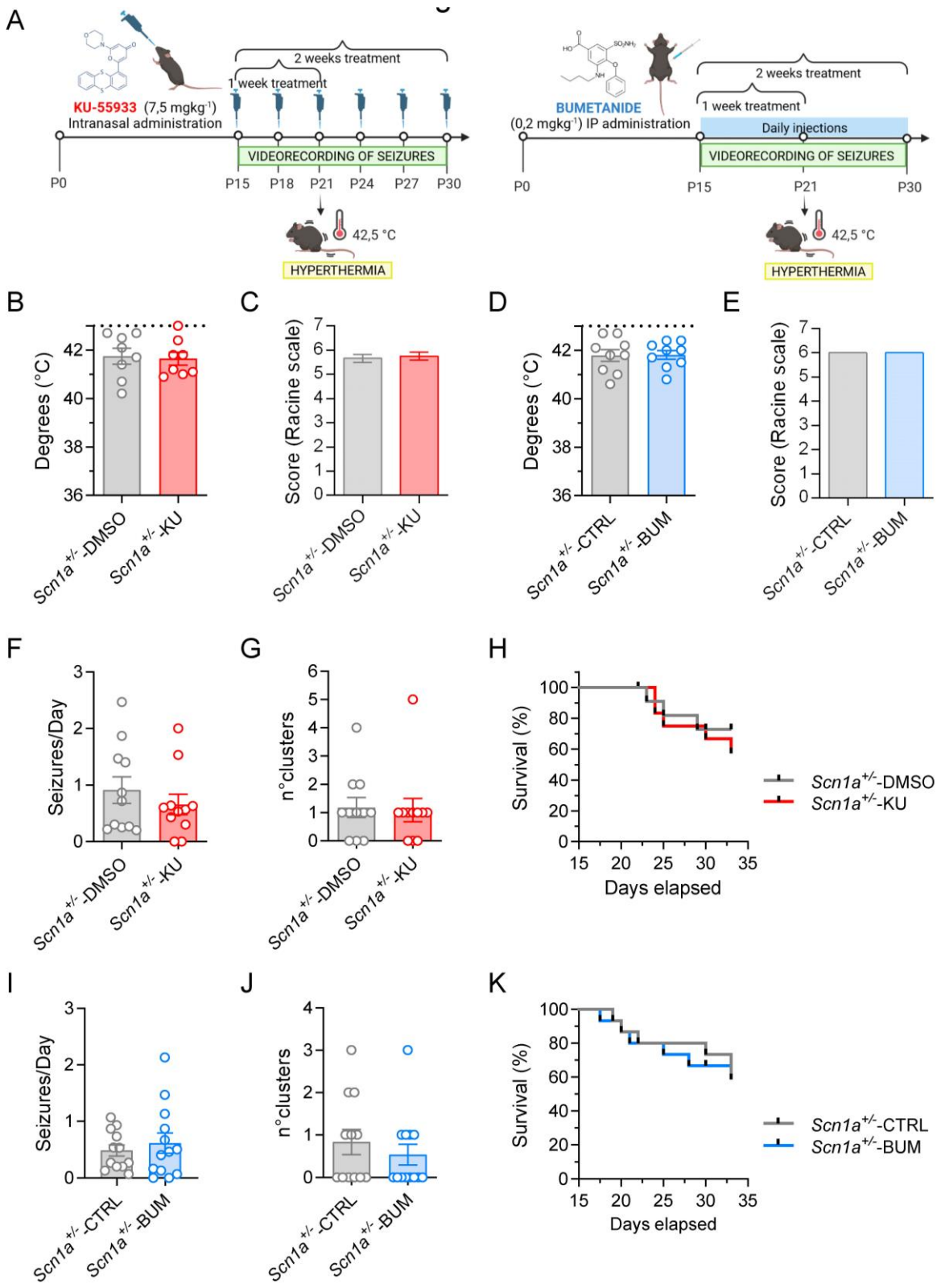


**Figure 3. KU and bumetanide treatments do not affect the epileptic phenotype of *Scn1a*$^{+/-}$ mice.**

**A.** Representative diagrams of KU55933 (KU) and Bumetanide (BUM) treatments and experimental timelines. Mice received KU 7.5 mg/kg intranasally every 72 hours or bumetanide 2 mg/kg IP daily starting from P15. The effect on hyperthermia induced seizures were assessed at P21 after a 1-week

treatment. The effect on spontaneous seizures was assessed in separated animal cohorts treated chronically for two weeks. **B, C.** Hyperthermia-induced seizures did not show any differences upon KU treatment, neither in the threshold temperature (*Scn1a*$^{+/-}$-DMSO, mean ± SEM = 41.75 ± 0.33°C, N = 8; *Scn1a*$^{+/-}$-KU mean ± SEM = 41.65 ± 0.26°C, N = 8; Mann-Whitney test, p-value = 0.7795) nor in the seizures' severity score (*Scn1a*$^{+/-}$-DMSO, mean ± SEM = 5.667 ± 0.1667, N = 8; *Scn1a*$^{+/-}$-KU mean ± SEM = 5.750 ± 0.1637, N = 8; Mann-Whitney test, p-value = >0.9999). **D, E**. Similar to KU, BUM did not affect neither the threshold temperature (*Scn1a*$^{+/-}$-CTRL mean ± SEM = 41.79 ± 0.24°C, N = 9; *Scn1a*$^{+/-}$-BUM mean ± SEM = 41.81 ± 0.17°C, N = 9; Mann-Whitney test, p-value = >0.9999) nor the severity score (*Scn1a*$^{+/-}$-CTRL mean ± SEM = 6 ± 0, N = 7; *Scn1a*$^{+/-}$-BUM mean ± SEM = 6 ± 0, N = 8, Mann-Whitney test, p-value = >0.9999). **F-G.** Video-analysis of spontaneous convulsive seizures showed no changes in KU-treated vs DMSO-treated mice in seizures' frequency (*Scn1a*$^{+/-}$-DMSO: mean ± SEM = 0.9127 ± 02363 seizures/day, N = 11; *Scn1a*$^{+/-}$-KU: mean ± SEM = 0.6573 ± 0.1818 seizures/day, N = 11; Mann-Whitney test, p-value = 0.6633) or number of clusters of seizures (*Scn1a*$^{+/-}$-DMSO: mean ± SEM = 1.182 ± 0.3521, N = 11; *Scn1a*$^{+/-}$-KU: mean ± SEM = 1.091 ± 0.4146, N = 11; Mann-Whitney test, p-value = 0.7575). **H.** KU did not improve the mortality rate (p-value = 0.9755 Kaplan-Meier). **I-J.** Similar to KU, Bumetanide treatment did not improve seizures' frequency (*Scn1a*$^{+/-}$-CTRL saline: mean ± SEM = 0.4833 ± 0.09969 seizures/day, N = 12; *Scn1a*$^{+/-}$-BUM: mean ± SEM = 0.6143 ± 0.1778 seizures/day, N = 13; Mann-Whitney test, p-value = 0.8831), clusters of seizures (*Scn1a*$^{+/-}$-CTRL saline: mean ± SEM = 83.33 ± 0.2973, N = 12; *Scn1a*$^{+/-}$-BUM: mean ± SEM = 0.5385 ± 0.2433, N = 13; Mann-Whitney test, p-value = 0.5005) (J). **K.** BUM treatment did not modify the mortality rate (p-value = 0.2356; Kaplan-Meier).

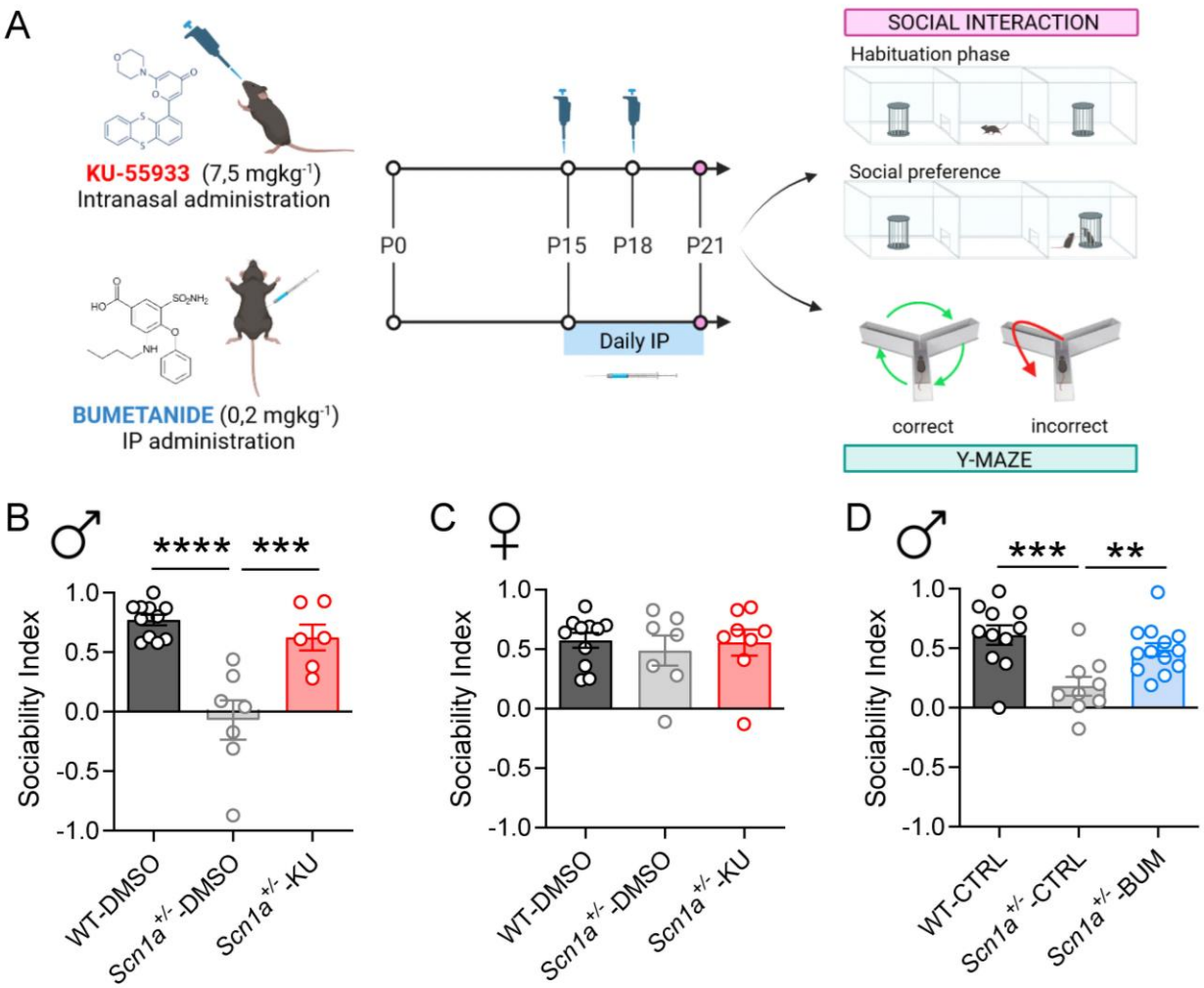


**Figure 4. KU and bumetanide treatments ameliorate sociability of *Scn1a*$^{+/-}$ mice.**

**A.** Diagram of the experimental timeline to test effects of KU55933 (KU) and bumetanide (BUM) on *Scn1a*$^{+/-}$ autistic-like phenotype. Animals received KU treatment (two intranasal administrations, at P15 and P18, spaced of 72 hours) or BUM treatment (one-week daily IP injections from P15). Three-chamber sociability test and Y-maze were performed at P21. **B.** *Scn1a*$^{+/-}$ male mice showed a defect in social preference compared to WT at P21, as indicated by a lower sociability index, and KU treatment rescued this alteration (WT-DMSO: mean ± SEM = 0.771 ± 0.044, N = 11; *Scn1a*$^{+/-}$- DMSO: mean ± SEM = -0.069 ± 0.165, N = 7; *Scn1a*$^{+/-}$- KU: mean ± SEM = 0.623 ± 0.109, N =6; One-Way ANOVA, Fisher's LSD post-hoc test, p-value: WT-DMSO vs Scn1a$^{+/-}$-DMSO = <0.0001, WT-DMSO vs. Scn1a$^{+/-}$-KU = 0.3208, Scn1a$^{+/-}$-DMSO vs. Scn1a$^{+/-}$-KU = 0.0003). **C.** The three-chamber test showed no defects in social interaction in *Scn1a*$^{+/-}$ females (WT-DMSO: mean ± SEM = 0.574 ± 0.062, N = 11; *Scn1a*$^{+/-}$- DMSO: mean ± SEM = 0.489 ± 0.126, N = 7; *Scn1a*$^{+/-}$- KU: mean ± SEM = 0.556 ± 0.110, N = 8, One-Way ANOVA, Fisher's LSD post-hoc test, p-value: WT-DMSO vs Scn1a$^{+/-}$-DMSO = 0.5269, WT-DMSO vs. Scn1a$^{+/-}$-KU = 0.8881, Scn1a$^{+/-}$-DMSO vs. Scn1a$^{+/-}$-KU = 0.6410). **D.** Like KU, BUM treatment

rescued defective sociability in *Scn1a*$^{+/-}$ male mice (WT-CTRL: mean ± SEM = 0.610 ± 0.082, N = 11; *Scn1a*$^{+/-}$-CTRL: mean ± SEM = 0.182 ± 0.079, N = 9; *Scn1a*$^{+/-}$- BUM: mean ± SEM = 0.488 ± 0.055, N = 13, One-Way ANOVA, Fisher's LSD post-hoc test, p-value: WT-CTRL vs Scn1a$^{+/-}$-CTRL = 0.0009, WT-CTRL vs. Scn1a$^{+/-}$-BUM = 0.2046, Scn1a$^{+/-}$-CTRL vs. Scn1a$^{+/-}$-BUM = 0.0252).

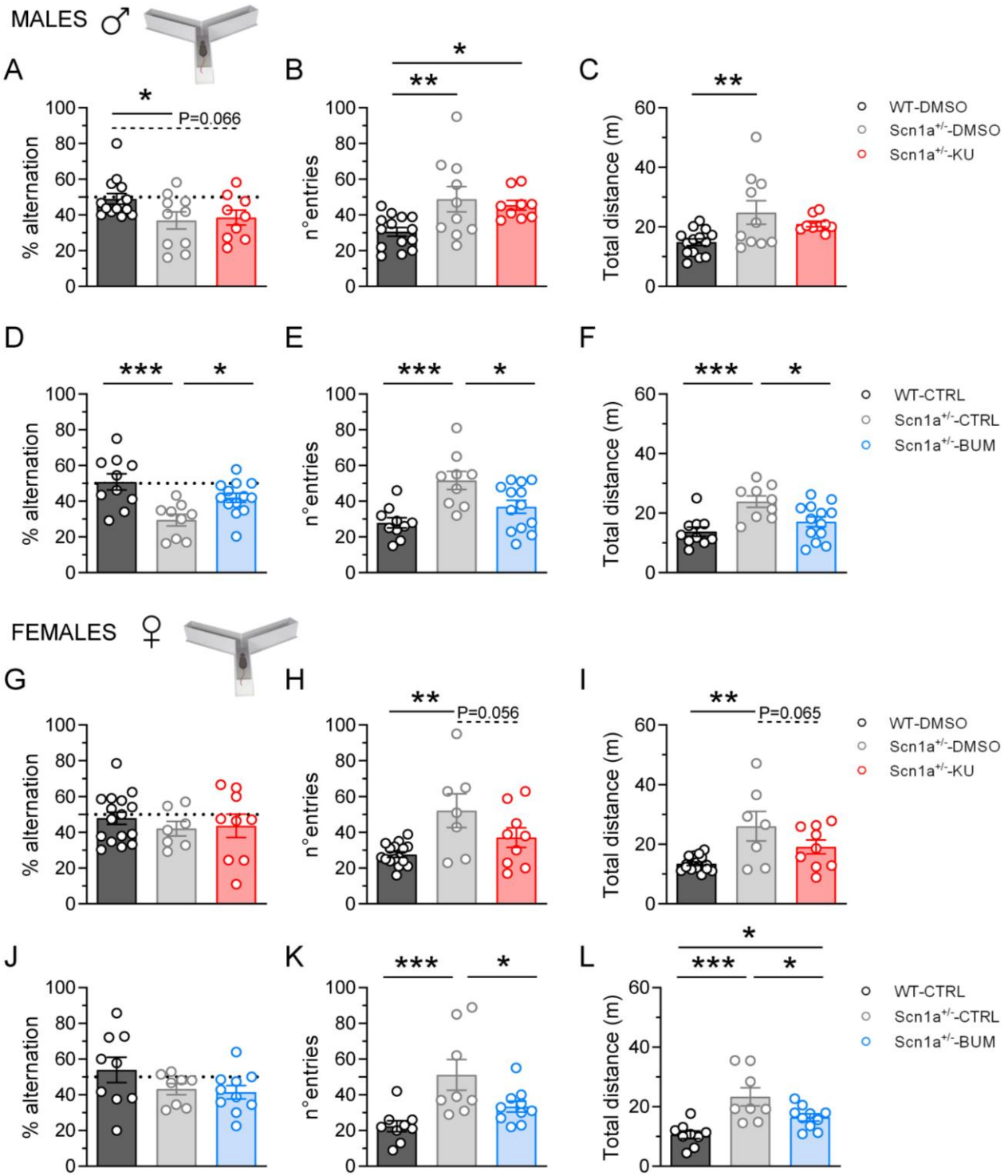


**Figure 5. Bumetanide, but not KU, improves Y-maze performance and decreases hyperactivity in *Scn1a*$^{+/-}$ mice.**

**A.** The Y-maze test showed a defect in spontaneous alternation in *Scn1a*$^{+/-}$ male mice compared to WT at P21. KU treatment did not show a clear rescue of this defect (WT-DMSO: mean ± SEM = 49.03 ± 2.98, N = 14; *Scn1a*$^{+/-}$- DMSO: mean ± SEM = 36.88 ± 4.79, N = 10; *Scn1a*$^{+/-}$- KU: mean ± SEM = 38.58 ± 4.18, N = 9; Fisher's LSD post-hoc test, p-value: WT-DMSO vs Scn1a$^{+/-}$-DMSO = 0.0295, WT-

DMSO vs. Scn1a$^{+/-}$-KU = 0.0664, Scn1a$^{+/-}$-DMSO vs. Scn1a$^{+/-}$-KU = 0.7748). **B.** KU-treated and control DMSO-treated *Scn1a$^{+/-}$* male mice displayed an increased number of entries in the maze during the test (WT-DMSO: mean ± SEM = 30.57 ± 2.46, N = 14; *Scn1a$^{+/-}$*- DMSO: mean ± SEM = 48.80 ± 7.13, N = 10; *Scn1a$^{+/-}$*- KU: mean ± SEM = 45.44 ± 2.71, N = 9; One-Way ANOVA, Fisher's LSD post-hoc test, p-value: WT-DMSO vs Scn1a$^{+/-}$-DMSO = 0.0046, WT-DMSO vs. Scn1a$^{+/-}$-KU = 0.0218, Scn1a$^{+/-}$-DMSO vs. Scn1a$^{+/-}$-KU = 0.6154). **C.** *Scn1a$^{+/-}$* male mice showed increased total distance compared to WT, and KU partially ameliorated this feature (WT-DMSO: mean ± SEM = 14.85 ± 1.14, N = 14; *Scn1a$^{+/-}$*-DMSO: mean ± SEM = 24.83 ± 3.98, N = 10; *Scn1a$^{+/-}$*- KU: mean ± SEM = 20.95 ± 0.90, N = 9; One-Way ANOVA, Fisher's LSD post-hoc test, p-value: WT-DMSO vs Scn1a$^{+/-}$-DMSO = 0.0034, WT-DMSO vs. Scn1a$^{+/-}$-KU = 0.0694, Scn1a$^{+/-}$-DMSO vs. Scn1a$^{+/-}$-KU = 0.2741). **D.** The control group of *Scn1a$^{+/-}$* male mice used for the bumetanide (BUM) treatment showed, similarly to the DMSO-control ones used for testing KU, a defect in spontaneous alternation compared to WT, which was rescued by BUM (WT-CTRL: mean ± SEM = 50.81 ± 4.55, N=10; *Scn1a$^{+/-}$*- CTRL: mean ± SEM = 29.48 ± 3.24, N=9; *Scn1a$^{+/-}$*- BUM: mean ± SEM = 41.96 ± 2.60, N=13; One-Way ANOVA, Fisher's LSD post-hoc test, p-value: WT-CTRL vs Scn1a$^{+/-}$-CTRL = 0.0003, WT-CTRL vs. Scn1a$^{+/-}$-BUM = 0.0719, Scn1a$^{+/-}$-CTRL vs. Scn1a$^{+/-}$-BUM = 0.0160). **E.** Control *Scn1a$^{+/-}$* male mice showed an increased number of entries which was rescued by BUM (WT-CTRL: mean ± SEM = 27.90 ± 2.795, N = 10; *Scn1a$^{+/-}$*- CTRL: mean ± SEM = 51.67 ± 5.069, N = 9; *Scn1a$^{+/-}$*- BUM: mean ± SEM = 36.85 ± 3.596, N = 13; One-Way ANOVA, Fisher's LSD post-hoc test, p-value: WT-CTRL vs Scn1a$^{+/-}$-CTRL = 0.0003, WT-CTRL vs. Scn1a$^{+/-}$-BUM = 0.1009, Scn1a$^{+/-}$-CTRL vs. Scn1a$^{+/-}$-BUM = 0.0109). **F.** Control *Scn1a$^{+/-}$* male mice showed an increased distance travelled, which was rescued by BUM (WT-CTRL: mean ± SEM = 13.77 ± 1.55, N = 10; *Scn1a$^{+/-}$*- CTRL: mean ± SEM = 23.85 ± 1.90, N = 9; *Scn1a$^{+/-}$*- BUM: mean ± SEM = 17.14 ± 1.68, N = 13; One-Way ANOVA, Fisher's LSD post-hoc test, p-value: WT-CTRL vs Scn1a$^{+/-}$-CTRL = 0.0005, WT-CTRL vs. Scn1a$^{+/-}$-BUM = 0.1646, Scn1a$^{+/-}$-CTRL vs. Scn1a$^{+/-}$-BUM = 0.0100). **G.** WT-DMSO , *Scn1a$^{+/-}$*-DMSO and *Scn1a$^{+/-}$*- KU female mice did not show differences in spontaneous alternation in the Y-maze test (WT-DMSO: mean ± SEM = 47.92 ± 3.41, N = 16; *Scn1a$^{+/-}$*- DMSO: mean ± SEM = 42.14 ± 4.09, N = 7; *Scn1a$^{+/-}$*- KU: mean ± SEM = 43.66 ± 6.55, N = 9; One-Way ANOVA, Fisher's LSD post-hoc test, p-value: WT-DMSO vs Scn1a$^{+/-}$-DMSO = 0.4047, WT-DMSO vs. Scn1a$^{+/-}$-KU = 0.5035, Scn1a$^{+/-}$-DMSO vs. Scn1a$^{+/-}$-KU = 0.8426). **H.** Female *Scn1a$^{+/-}$* mice, as male ones, showed an increased number of entries in the Y-maze, with a trend towards rescue upon KU treatment (WT-DMSO: mean ± SEM = 27.63 ± 1.52, N = 16; *Scn1a$^{+/-}$*- DMSO: mean ± SEM = 52.14 ± 9.50, N = 7; *Scn1a$^{+/-}$*- KU: mean ± SEM = 37.11 ± 5.48, N = 9; One-Way ANOVA, Fisher's LSD post-hoc test, p-value: WT-DMSO vs

Scn1a$^{+/-}$-DMSO = 0.0011, WT-DMSO vs. Scn1a$^{+/-}$-KU = 0.1394, Scn1a$^{+/-}$-DMSO vs. Scn1a$^{+/-}$-KU = 0.0560). **I.** Female *Scn1a$^{+/-}$* mice, as male ones, showed increased total distance travelled during the Y-maze test, with a trend towards rescue upon KU treatment (WT-DMSO: mean ± SEM = 13.50 ± 0.61, N = 16; *Scn1a$^{+/-}$*- DMSO: mean ± SEM = 26.06 ± 4.94, N = 7; *Scn1a$^{+/-}$*- KU: mean ± SEM = 19.11 ± 2.33, N = 9 Fisher's LSD post-hoc test, p-value: WT-DMSO vs Scn1a$^{+/-}$-DMSO = 0.0006, WT-DMSO vs. Scn1a$^{+/-}$-KU = 0.0718, Scn1a$^{+/-}$-DMSO vs. Scn1a$^{+/-}$-KU = 0.0657). **J.** As in the KU experimental cohort, Y-maze test showed no differences in Y-maze performance in WT, *Scn1a$^{+/-}$*- CTRL and *Scn1a$^{+/-}$*- CTRL female mice (WT-CTRL: mean ± SEM = 53.98 ± 7.04, N = 9; *Scn1a$^{+/-}$*- CTRL: mean ± SEM = 43.23 ± 3.15, N = 8; *Scn1a$^{+/-}$*- BUM: mean ± SEM = 42.75 ± 3.60, N = 10; One-Way ANOVA, Fisher's LSD post-hoc test, p-value: WT-CTRL vs Scn1a$^{+/-}$-CTRL = 0.1523, WT-CTRL vs. Scn1a$^{+/-}$-BUM = 0.0808, Scn1a$^{+/-}$-CTRL vs. Scn1a$^{+/-}$-BUM = 0.8037). **K.** BUM rescued the increased number of entries showed by *Scn1a$^{+/-}$* mice during the Y-maze test (WT-CTRL: mean ± SEM = 22.44 ± 3.09, N = 9; *Scn1a$^{+/-}$*- CTRL: mean ± SEM = 51.13 ± 8.60, N = 8; *Scn1a$^{+/-}$*- BUM: mean ± SEM = 36.09 ± 3.85, N = 10; Fisher's LSD post-hoc test, p-value: WT-CTRL vs Scn1a$^{+/-}$-CTRL = 0.0008, WT-CTRL vs. Scn1a$^{+/-}$-BUM = 0.1335, Scn1a$^{+/-}$-CTRL vs. Scn1a$^{+/-}$-BUM = 0.0228). **L.** The increased total distance travelled by *Scn1a$^{+/-}$* mice during the Y-maze test was partially reduced by BUM but was still different from WT (WT-CTRL: mean ± SEM = 10.61 ± 1.28, N = 9; *Scn1a$^{+/-}$*- CTRL: mean ± SEM = 23.34 ± 3.05, N = 8; *Scn1a$^{+/-}$*- BUM: mean ± SEM = 17.70 ± 1.67, N = 10; One-Way ANOVA, Fisher's LSD post-hoc test, p-value: WT-CTRL vs Scn1a$^{+/-}$-CTRL = 0.0001, WT-CTRL vs. Scn1a$^{+/-}$-BUM = 0.0346, Scn1a$^{+/-}$-CTRL vs. Scn1a$^{+/-}$-BUM = 0.0165).

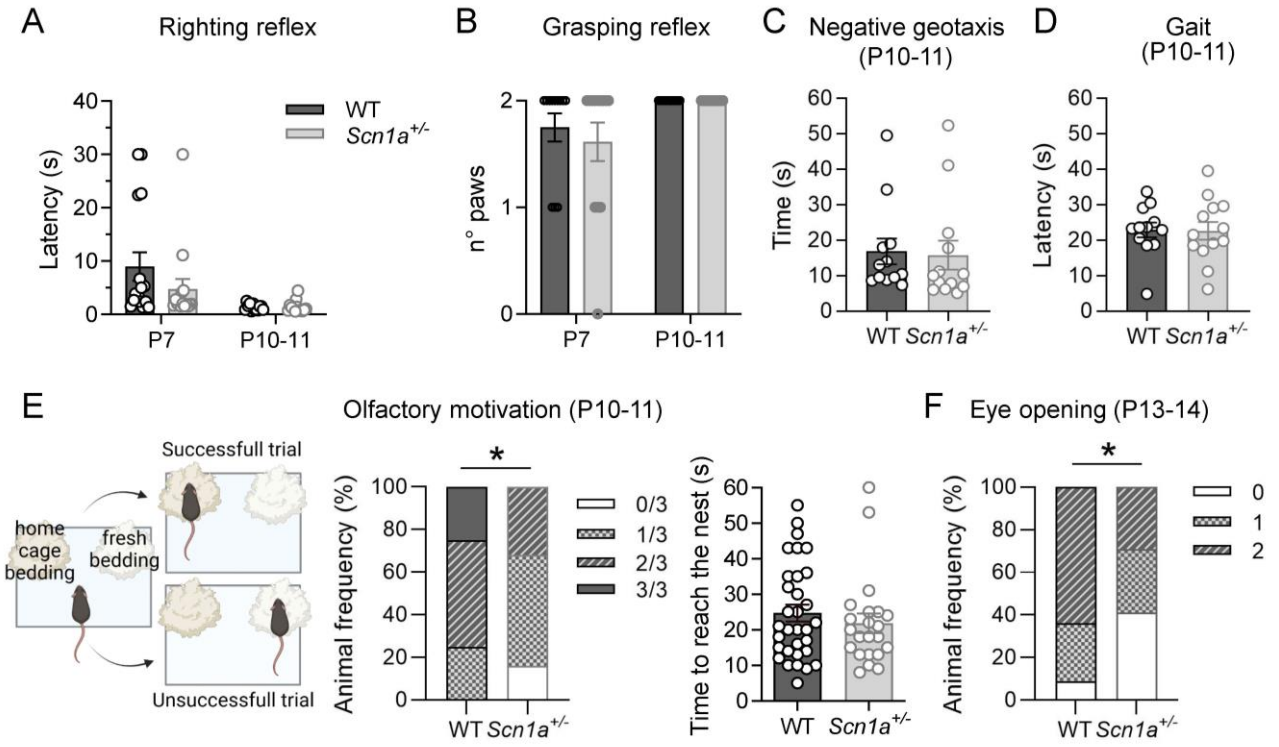


**Figure 6. Early neurodevelopmental characterization of *Scn1a*$^{+/-}$ mice.**

**A.** Righting reflex analysis (cut-off 30 s) did not show any differences between WT and *Scn1a*$^{+/-}$ mice at P7 (WT: mean ± SEM = 8.98 ± 2.65, N = 16; *Scn1a*$^{+/-}$: mean ± SEM = 4.73 ± 1.91, N = 15) or P10-11 (WT: mean ± SEM = 1.37 ± 0.17, N = 12; *Scn1a*$^{+/-}$: mean ± SEM = 1.45 ± 0.30, N = 13); Mann-Whitney test, p-value: P7 = 0.0723, P10-11 >0.9999. **B.** Grasping reflex test (forepaws) did not show any differences between WT and *Scn1a*$^{+/-}$ mice at P7 (WT, N=12; *Scn1a*$^{+/-}$, N = 13) or P10-11 (WT, N = 12; *Scn1a*$^{+/-}$, N = 13); Chi-square test, p-value: P7 = 0.6183, P10-11 = 1.0000. **C.** The negative geotaxis test at P10-11 gave similar results for *Scn1a*$^{+/-}$ and WT mice (WT: mean ± SEM = 16.84 ± 3.66, N=12; *Scn1a*$^{+/-}$: mean ± SEM = 15.80 ± 4.08, N = 13); Mann-Whitney test, p-value = 0.3435. **D.** The gait test showed no differences between *Scn1a*$^{+/-}$ and WT mice at P10-11 (WT: mean ± SEM = 22.89 ± 2.10, N = 12; *Scn1a*$^{+/-}$: mean ± SEM = 22.65 ± 2.49, N = 13); Mann-Whitney test, p-value = 0.7391. **E.** *Scn1a*$^{+/-}$ mice showed dysfunctions in the nest bedding test (olfactory motivation) compared with WT at P10-11. Three trials for each animal were performed and considered successful if the animal reached the nest bedding in less than 60 s. The number of animals succeeding in 0, 1, 2 or 3 trials were compared between WT (N = 16) and *Scn1a*$^{+/-}$ (N = 19) mice; chi-square test, P = 0.022. The time needed to reach the nest was similar for the two genotypes; (WT: mean ± SEM = 24.75 ± 2.39; *Scn1a*$^{+/-}$: mean ± SEM = 21.86 ± 2.73); Mann-Whitney test, p-value = 0.4651. **F.** Eye opening is delayed in *Scn1a*$^{+/-}$ (N = 17) compared with WT (N = 22) mice (number of animals with 0, 1 or 2 open eyes at P13-14); chi-square test, P = 0.037.

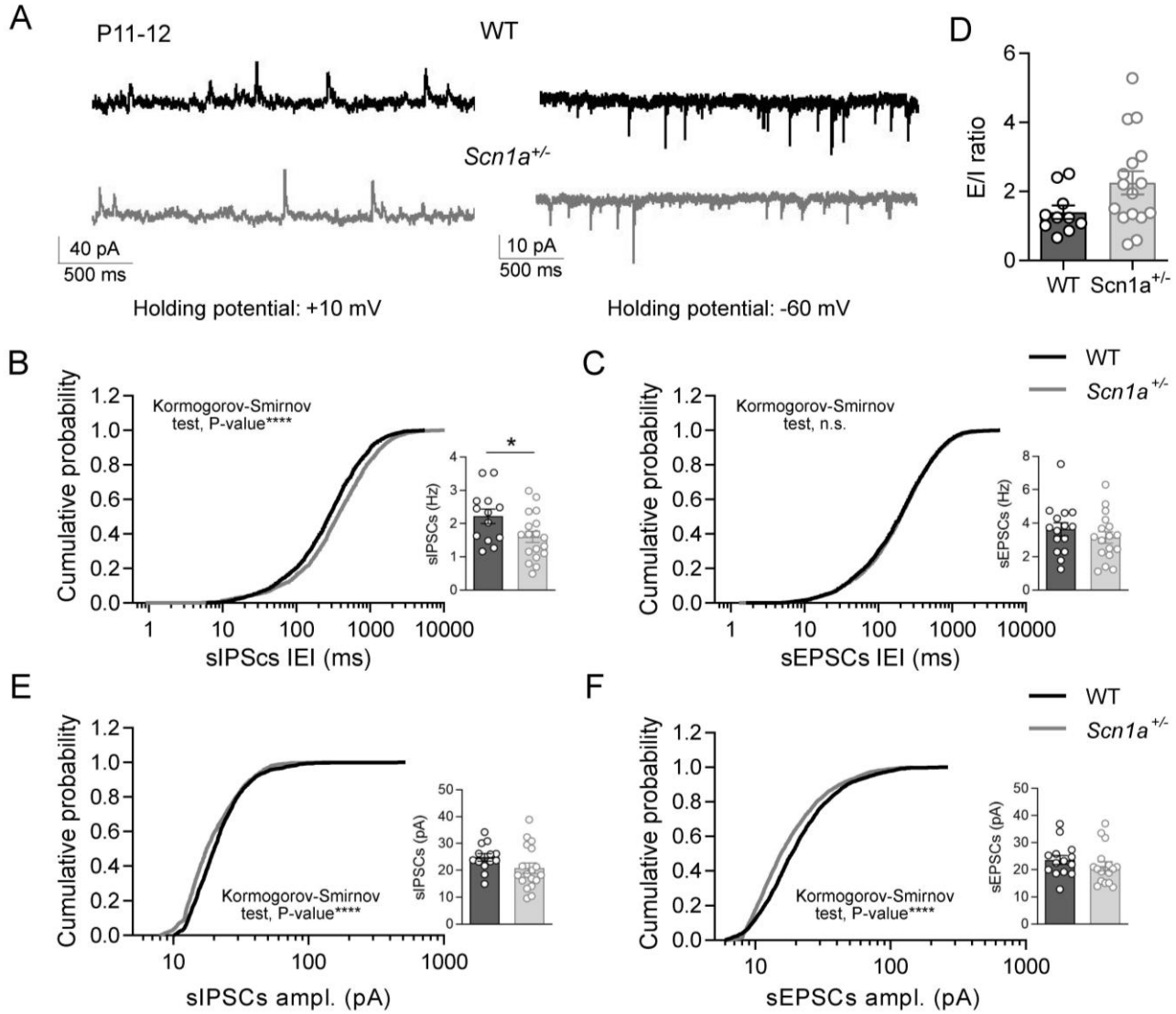


**Figure 7. *Scn1a*$^{+/-}$ mice show defects in spontaneous synaptic activity before seizures appearance.** **A.** Representative traces of spontaneous GABAergic post-synaptic currents (sIPSCs) and glutamatergic post-synaptic currents (sEPSCs) recorded in P10-12 hippocampal CA1 pyramidal neurons clamped at +10 mV and -60 mV, respectively. **B.** The cumulative distribution of sIPSCs inter event interval (IEI) revealed an increase in *Scn1a*$^{+/-}$ mice compared to WT, KS test p-value <0.0001. Consistently, the analysis of mean synaptic events showed a decreased frequency of sIPSCs in *Scn1a*$^{+/-}$ mice (mean ± SEM = 1.60 ± 0.17, n = 18 cells, N = 3 animals) compared to WT (mean ± SEM = 2.22 ± 0.22, n = 13 cells, N = 3 animals), unpaired t-test, P = 0.0301. **C.** Cumulative distribution of sEPSCs IEI revealed no changes in *Scn1a*$^{+/-}$ compared to WT mice, KS test. Similarly, there were no changes in sEPSCs mean frequency in *Scn1a*$^{+/-}$ (mean ± SEM = 3.15 ± 0.34, n = 17 cells, N = 3 animals) compared to WT (mean ± SEM = 3.63 ± 0.39, n=15 cells, N = 3 animals) mice, unpaired t-test, p-value = 0.3591. **D.** The excitatory/inhibitory ratio (E/I) has been obtained dividing sEPSCs and sIPSCs frequencies measured in the same neuron (WT: mean ± SEM = 1.398 ± 0.1957, n = 10 cells, N = 3

animals; *Scn1a*$^{+/-}$: mean ± SEM = 2.251 ± 0.3375, n = 16 cells, N = 3 animals). Unpaired t-test, P = 0.0741. **E.** The cumulative distribution of sIPSCs amplitudes revealed a slight decrease in *Scn1a*$^{+/-}$ mice (n = 18 cells, N = 3 animals) compared to WT (n = 13 cells, N = 3 animals), KS test p-value <0.0001, which did not reach statistical significance comparing mean values (WT: mean ± SEM = 24.80 ± 1.41; *Scn1a*$^{+/-}$: mean ± SEM = 20.77 ± 1.90); unpaired t-test, p-value = 0.1243. **F.** Cumulative distribution of sEPSCs amplitude revealed a decrease in *Scn1a*$^{+/-}$ (n = 17 cells, N = 3 animals) compared to WT (n = 14 cells, N = 3 animals) mice, KS test p-value <0.0001, which did not reach statistical significance comparing mean values (WT: mean ± SEM = 23.59 ± 1.68; *Scn1a*$^{+/-}$: mean ± SEM = 21.27 ± 1.66); unpaired t-test, p-value = 0.3400.

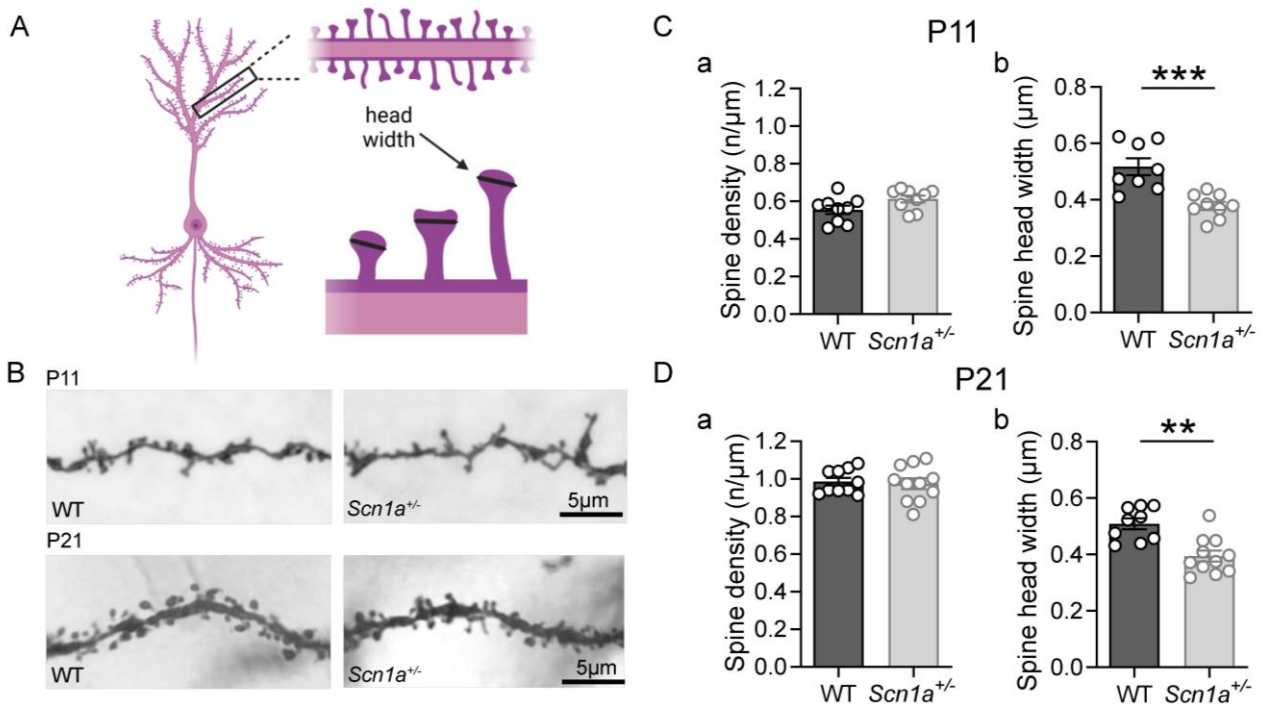


**Figure 8. *Scn1a*$^{+/-}$ mice show defects in spine maturation.**

**A.** Representation of dendritic spines in CA1 pyramidal cell and illustration of how the morphometric parameter "head width" was quantified (black segments in the spine heads). **B.** Representative images of dendritic spines of pyramidal neurons in the CA1 area of the hippocampus of P11 (upper panels) and P21 (lower panels) in WT and *Scn1a*$^{+/-}$ mice (Golgi staining). **C(a).** No change in spine density between WT (mean ± SEM = 0.5546 ± 0.02270; N = 9 mice) and *Scn1a*$^{+/-}$ (mean ± SEM = 0.6120 ± 0.01862; N mice = 9) P11 mice. Mann-Whitney test, p-value = 0.0767. **C(b).** Decreased spine head width in *Scn1a*$^{+/-}$ mice at P11. WT (mean ± SEM = 0.5173 ± 0.03001; N = 8 mice) and *Scn1a*$^{+/-}$ (mean ± SEM = 0.3787 ± 0.01432; N = 9 mice). Mann-Whitney test, p-value = 0.0006. **D(a).** No change in spine density in P21 *Scn1a*$^{+/-}$ mice (mean ± SEM = 0.9748 ± 0.02860; N =11 mice) compared with WT (mean ± SEM = 0.9855 ± 0.02019; N = 10 mice). Mann-Whitney test, p-value = 0.9017. **D(b).** Decreased spine head width in *Scn1a*$^{+/-}$ mice at P21. WT (mean ± SEM = 0.5084 ± 0.01938; N = 9 mice) and *Scn1a*$^{+/-}$ (mean ± SEM = 0.3944 ± 0.01959; N = 11 mice) mice. Mann-Whitney test, p-value = 0.0016.